
Robustness Disparities in Face Detection

Samuel Dooley¹, George Z. Wei², Tom Goldstein¹, John P. Dickerson¹

¹University of Maryland

²University of Massachusetts Amherst

{sdooley1, tomg, john}@cs.umd.edu, gzwei@umass.edu

Abstract

Facial analysis systems have been deployed by large companies and critiqued by scholars and activists for the past decade. Many existing algorithmic audits examine the performance of these systems on later stage elements of facial analysis systems like facial recognition and age, emotion, or perceived gender prediction; however, a core component to these systems has been vastly understudied from a fairness perspective: face detection, sometimes called face localization. Since face detection is a pre-requisite step in facial analysis systems, the bias we observe in face detection will flow downstream to the other components like facial recognition and emotion prediction. Additionally, no prior work has focused on the robustness of these systems under various perturbations and corruptions, which leaves open the question of how various people are impacted by these phenomena. We present the first of its kind detailed benchmark of face detection systems, specifically examining the robustness to noise of commercial and academic models. We use both standard and recently released academic facial datasets to quantitatively analyze trends in face detection robustness. Across all the datasets and systems, we generally find that photos of individuals who are *masculine presenting*, *older*, of *darker skin type*, or have *dim lighting* are more susceptible to errors than their counterparts in other identities.

1 Introduction

Face detection identifies the presence and location of faces in images and video. In this work, face detection, also called face localization, refers to the task of placing a rectangle around the location of all faces in an image. Automated face detection is a core component of myriad systems—including *face recognition technologies* (FRT), wherein a detected face is matched against a database of faces, typically for identification or verification purposes. FRT-based systems are widely deployed [11, 33, 74]. Automated face recognition enables capabilities ranging from the relatively morally neutral (e.g., searching for photos on a personal phone [27]) to morally laden (e.g., widespread citizen surveillance [33], or target identification in warzones [51]). Legal and social norms regarding the usage of FRT are evolving [e.g., 28]. For example, in June 2021, the first county-wide ban on its use for policing [see, e.g., 24] went into effect in the US [29]. Some use cases for FRT will be deemed socially repugnant and thus be either legally or *de facto* banned from use; yet, it is likely that pervasive use of facial analysis will remain—albeit with more guardrails than today [67].

One such guardrail that has spurred positive, though insufficient, improvements and widespread attention is the use of benchmarks. For example, in late 2019, the US National Institute of Standards and Technology (NIST) adapted its venerable Face Recognition Vendor Test (FRVT) to explicitly include concerns for demographic effects [28], ensuring such concerns propagate into industry systems. Yet, differential treatment by FRT of groups has been known for at least a decade [e.g., 21, 41], and more recent work spearheaded by [8] uncovers unequal performance at the phenotypic

subgroup level. That latter work brought widespread public, and thus burgeoning regulatory, attention to bias in FRT [e.g., 39, 48].

One yet unexplored benchmark examines the bias present in a model’s robustness (e.g., to noise, or to different lighting conditions), both in aggregate and with respect to different dimensions of the population on which it will be used. Many detection and recognition systems are not built in house, instead adapting an existing academic model or by making use of commercial cloud-based “ML as a Service” (MLaaS) platforms offered by tech giants such as Amazon, Microsoft, Google, Megvii, etc. With this in mind, our **main contribution** is a wide *robustness benchmark* of six different face detection models, three commercial-grade face detection systems (accessed via Amazon’s Rekognition, Microsoft’s Azure, and Google Cloud Platform’s face detection APIs) and three high-performing academic face detection models (MogFace, TinaFace, and YOLO5Face). For fifteen types of realistic noise, and five levels of severity per type of noise [35], we test all models against images in each of four well-known datasets. Across these more than 5,000,000 noisy images from four commonly used academic datasets: Adience [20], Casual Conversations Dataset [34], MIAP [65], and UTKFace [82]. Additionally, to allow further research, we make our raw data available for exploration here: <https://dooleys.github.io/robustness/>.¹

By benchmarking both commercial and academic models, we can understand two important insights: (1) audit the use-case of a company which takes open-source models to build in-house facial recognition models, and (2) adjudicate corporation’s claims of caring about demographic biases in their products by measuring the extent to which their models are less biased than academic models which have no fairness considerations. As such, we endeavor to answer three research questions:

- (RQ1):** How robust are commercial and academic face detection models to natural types of noise?
- (RQ2):** Do face detection models have demographic disparities in their performance on natural noise robustness tasks?
- (RQ3):** Are the robustness disparities exhibited by commercial models more or less than the robustness disparities exhibited by academic models?

To answer these questions, we are motivated to understand how natural perturbations change the **system output**. We statistically analyze the performance of three common commercial facial detection providers and three state-of-the-art academic face detection models, comparing their performance and demographic disparities by comparing the output of the system on an unperturbed image with the output on a perturbed version of that image. This is interesting because it isolates the impact of the noise on the system, independent of the performance of the system. Thus, it makes comparing across systems easier. Focusing on **output** instead of system **performance** better isolates the impact of the stimulus of interest – the noise.

We observe that (RQ1) the leading face detection models show varying degrees of robustness to natural noise, but generally perform poorly on this task. Further, we conclude that (RQ2) these models do have demographic disparities which are statistically significant, and show a bias against individuals who are older, present as masculine, are darker skinned, and are dimly lit. Additionally, we see that (RQ3) these biases align with the commercial models, but that commercial model generally do not have lower level of disparity than the academic models.

Overall, our results suggest that regardless of a commercial company’s commitments to equal treatment of different demographic groups, there are still pernicious problems with their products which treat demographic groups differently. We see further evidence that face detection is less robust to noise on older and masculine presenting individuals, which calls for future efforts to address this systemic problem. While our work indicates that the commercial providers are no worse on this important and socially impactful task than academics, we would hope to see that the commitments made by commercial companies would have them dedicate their vast resources and access to do better than comparatively under-resourced academics and substantially improve upon the robustness of their widely-used systems.

2 Related Work

We briefly overview additional related work in the two core areas addressed by our benchmark: robustness to noise and demographic disparity in facial detection and recognition. That latter point

¹This work combines two unpublished papers which we wrote previously: [14] and [15]. This submission expands on those papers’ ideas and enhances them with more rigorous analysis.

overlaps heavily with the fairness in machine learning literature; for additional coverage of that broader ecosystem and discussion around bias in machine learning writ large, we direct the reader to survey works due to [10] and [3].

Demographic effects in facial detection and recognition. The existence of differential performance of facial detection and recognition on groups and subgroups of populations has been explored in a variety of settings [8, 28, 37, 41, 56, 61]. In this work, we focus on *measuring* the impact of noise on a classification task, like that of [75]; indeed, a core focus of our benchmark is to *quantify* relative drops in performance conditioned on an input datapoint’s membership in a particular group. We view our work as a *benchmark*, that is, it focuses on quantifying and measuring, decidedly not providing a new method to “fix” or otherwise mitigate issues of demographic inequity in a system. Toward that latter point, existing work on “fixing” unfair systems can be split into three (or, arguably, four [64]) focus areas: pre-, in-, and post-processing. Pre-processing work largely focuses on dataset curation and preprocessing [e.g., 22, 60, 63, 71]. In-processing often constrains the ML training method or optimization algorithm itself [e.g., 2, 12, 13, 26, 42, 52, 57, 71, 78, 79, 80], or focuses explicitly on so-called fair representation learning [e.g., 1, 5, 18, 19, 49, 72, 81]. Post-processing techniques adjust decisioning at inference time to align with quantitative fairness definitions [e.g., 32, 73].

Robustness to noise. Quantifying, and improving, the robustness to noise of face detection and recognition systems is a decades-old research challenge. Indeed, mature challenges like NIST’s Facial Recognition Vendor Test (FRVT) have tested for robustness since the early 2000s [58]. We direct the reader to a comprehensive introduction to an earlier robustness challenge due to NIST [59]; that work describes many of the specific challenges faced by face detection and recognition systems, often grouped into Pose, Illumination, and Expression (PIE). It is known that commercial systems still suffer from degradation due to noise [e.g., 36]; none of this work also addresses the intersection of noise with bias, as we do.

Recently, *adversarial* attacks have been proposed that successfully break commercial face recognition systems [9, 66]; we note that our focus is on *natural* noise, as motivated by [35] with their ImageNet-C benchmark. Literature at the intersection of adversarial robustness and fairness is nascent and does not address commercial platforms [e.g., 54, 68]. To our knowledge, our work is the first systematic benchmark for commercial face detection systems that addresses, comprehensively, noise and its differential impact on (sub)groups of the population.

Academic Face Detection Models. Since 2012, neural-network-based face detectors have become ubiquitous in both industry and academia due to their comparative advantage in model capacity over traditional methods. As such, we are only going to focus on the prevailing approaches in deep face detection. According to Minaee et al. [53], there are five main categories of face detectors. *Cascade-CNN Based Models* generally use convolutional neural networks (CNNs) that operate at various resolutions to produce detections that are then repeatedly refined (or “cascaded”) through non-maximum suppression and bounding box regression to ultimately output final face detections [44]. *R-CNN Based Models* utilize a region proposal network to predict face regions and landmarks and then verify that the candidate regions are faces or not with a Regional CNN [25]. *Single Shot Detector (SSD) Models* discretize the output space of bounding boxes over different aspect ratios as well as scales then use the confidence scores to reshape the default boxes to better contain the detected faces by using convolutional features from different layers, usually the higher level layers [47]. *Feature Pyramid Network (FPN) Based Models* upsample the convolutional features of higher (semantically richer) layers, aggregates them with those calculated in the initial forward pass to create semantically rich features at all image scales, then detects faces with each of these features at each layer [46]. *Transformers Based Models* use the Transformer [70] (or the Vision Transformer [16]) as the backbone for face detection. The academic models evaluated in this paper fall into the FPN or SSD based detector categories and were chosen because they were top performers of the popular WIDER FACE [76, 77] benchmark.

Our work is most closely related to that of [38], who look at *adversarial noise* and how that effects “gender detection”, “age prediction”, and “smile detection”. [38] explicitly do not examine detection as defined by face localization, which is the topic of this study. Further, their facial analysis technologies generally are downstream processes from the facial detection/localization technology in this paper. Additionally, [50] provide a similar experimental design as our work though for face verification, and on a significantly smaller set of image distortions and test images. We refer the reader to [69] and [17] for surveys on bias in facial processing and biometrics.



Figure 1: Our benchmark consists of 5,066,312 images of the 15 types of algorithmically generated corruptions produced by ImageNet-C. We use data from four datasets (Adience, CCD, MIAP, and UTKFace) and present examples of corruptions from each dataset here.

3 Benchmark Design

In this section, we outline the details of our benchmark by describing the data we used, the protocol or method we employed to answer our research questions, and the evaluation metric. We also describe how our benchmark can be used by other researchers, the limitations of our benchmark, and give an important social context for our study in facial analysis technology.

Datasets This benchmark uses four datasets to evaluate the robustness of three commercial and three academic face detection models. The datasets are described below.

The Open Images Dataset V6 – Extended; More Inclusive Annotations for People (**MIAP**) dataset [65] was released by Google in May 2021 as an extension of the popular, permissive-licensed Open Images Dataset specifically designed to improve annotations of humans. For each image, every human is exhaustively annotated with bounding boxes for the entirety of their person visible in the image. Each annotation also has perceived gender (Feminine/Masculine/Unknown) presentation and perceived age (Young, Middle, Old, Unknown) presentation.

The Casual Conversations Dataset (**CCD**) [34] was released by Facebook in April 2021 under limited license and includes videos of actors. Each actor consented to participate in an ML dataset and provided their self-identification of age and gender identity (coded as Female, Male, and Other), each actor’s skin type was rated on the Fitzpatrick scale [23], and each video was rated for its ambient light quality. For our benchmark, we extracted one frame from each video.

The **Adience** dataset [20] under a CC license, includes cropped images of faces from images “in the wild”. Each cropped image contains only one primary, centered face, and each face is annotated by an external evaluator for age and perceived gender (Female/Male). The ages are reported as member of 8 age range buckets: 0-2; 3-7; 8-14; 15-24; 25-35; 36-45; 46-59; 60+.

Finally, the **UTKFace** dataset [82] under a non-commercial license, contains images with one primary subject with annotated for age (continuous), perceived gender (Female/Male), and ethnicity (White/Black/Asian/Indian/Others) by an algorithm, then checked by human annotators.

For each of the datasets, we randomly selected a subset of images for our evaluation, with caps on the number of images from each intersectional identity equal to 1,500. This reduces the effect of highly imbalanced datasets. We include a total of 66,662 clean images with 14,919 images from Adience; 21,444 images from CCD; 8,194 images from MIAP; and 22,105 images from UTKFace. The full breakdown of totals of images from each group can be found in Section A.2.

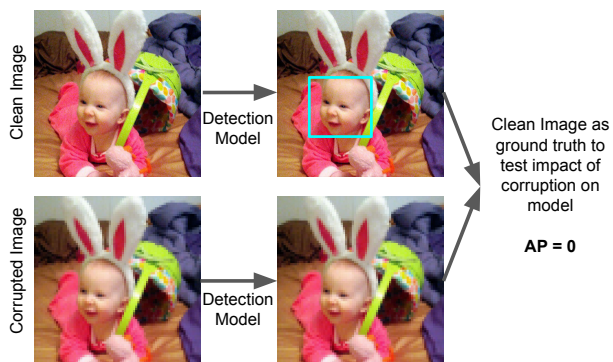


Figure 2: Depiction of how Average Precision (AP) metric is calculated by using clean image as ground truth.

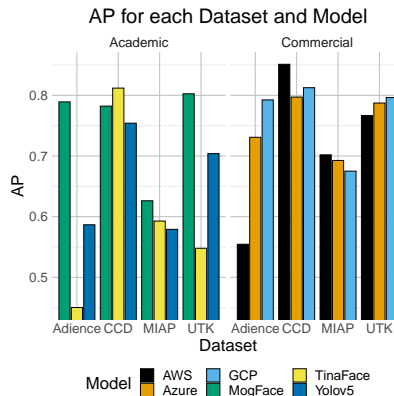


Figure 3: Overall performance (AP) of each model on each dataset.

Benchmark Protocol and Metrics. Recall, our motivating question is how the noise impacts a model’s output. To do this, each image was corrupted a total of 75 times, per the ImageNet-C protocol with the main 15 corruptions each with 5 severity levels. Examples of these corruptions can be seen in Figure 1. This resulted in a total of 5,066,312 images (including the original clean ones) which were each passed through each of the six models. Images were processed and stored within AWS’s cloud using S3 and EC2. The experiments cost was \$17,507.55 and a breakdown can be found in Appendix C.

We evaluate the change of the face systems under perturbations using the standard object detection metric: mean average precision (mAP). We use the standard implementation of the mAP metric by COCO [45]. Values reported below are mAP scores averaged over intersection over union (IoU) thresholds between 0.5 and 0.95 in intervals of 0.05. Below we call this metric Average Precision because we only have one class so the “mean” in mean average precision is trivial. Since we are interested in the system change under perturbation, and because none of the datasets have underlying ground truths, we treat the system output of the clean image as ground truth. A visual depiction of this process can be found in Figure 2.

We also investigate the significance of whether two groups are equally treated by a model under each metric by performing statistical tests. We observe bias by first performing a Kruskal-Wallis Rank Sum Test between explanatory and response variables which indicate whether two or more groups are treated equally or not. In the case where there is enough evidence to show that groups are treated differently, we then run the Pairwise Wilcoxon Rank Sum Tests to observe which groups have significantly different treatment and in which direction. All statistical tests are reported with $\alpha = 0.05$ with Bonferroni-Holm corrections. Each claim we make across datasets is done by looking at the trends in each dataset and are inherently qualitative.

We visually represent our results in Figures 4-7 by examining odds ratios between two categories of a sociodemographic variable across each model and dataset. For each pair of subgroups, like Middle-aged and Older subjects in Figure 5, we calculate the odds of each for each subgroup, $Odds_{middle}$ and $Odds_{older}$ and then look at their ratio: $Odds_{middle}/Odds_{older}$. When this value is greater than 1, like in Figure 5, it means the odds of higher performance are larger for middle aged group is higher than the older group. We conclude that there is a bias against older subjects. When the error bounds do not cross 1, this means that this disparity is statistically significant as well.

How to Use our Benchmark. There are three main ways that our benchmark could be used by future researchers and practitioners. First, the analysis code, data, and results are being released publicly. New models that are built, either in academia or industry, can be easily benchmarked against our framework, and progress in this space can be tracked by the research community. Indeed, it is our intention to communicate our results to standards bodies such as NIST for inclusion in, or influence on, their long-running FRVT gauntlet. Second, the comparison across types of models (in our case, academic and commercial) could be adopted by more algorithmic audits. For example, in many areas (language models for text generation, diffusion models for text to image tasks, myriad object detection tasks) academic, industry-funded but open-sourced, and industry-funded and closed-source models compete across various metrics, and comparing and contrasting appropriately-defined bias metrics

across those verticals is of practical importance. Third, well-founded and quantitative studies may be of use to policymakers. As discussed in Section 1, facial analysis is a topic of great regulatory and legislative interest at this moment, and informing all sides—policymakers, the public, and providers of facial analysis technology—will lead to more clear and educated discussion and norm setting.

What is not included in this study. There are three main things that this benchmark does not address. First, we do not examine cause and effect. We report inferential statistics without discussion of what generates them. Second, we only examine the types of algorithmically generated natural-like noise present in the 15 corruptions. We explicitly do not study or measure robustness to other types of changes to images, for instance adversarial noise, camera dimensions, etc. Finally, we do not investigate algorithmic training. We do not assume any knowledge of how the commercial system was developed or what training procedure or data were used.

Social Context. This benchmark relies on socially constructed concepts of gender presentation and skin-tone/race and the related concept of age. While this benchmark analyzes phenotypal versions of these from metadata on ML datasets, it would be wrong to interpret our findings absent a social lens of what these demographic groups mean inside a society. We guide the reader to Benthall and Haynes [4] and Hanna et al. [31] for a look at these concepts for race in machine learning, and Hamidi et al. [30] and Keyes [40] for similar looks at gender.

4 Results

4.1 RQ1: Overall Model Performance

To answer RQ1 and to provide a baseline for comparison later in the analysis, we examine the overall performance of each model on each dataset, presented in Figure 3. We see from the outset that we can answer RQ1 affirmatively: face detection models sometimes struggle significantly with robustness to noise. Commercial models as a whole outperform the academic models on every dataset – however there are individual models in each category which break this conclusion. For example, the academic model MogFace performs significantly better than all the commercial models on UTKFace, though as a whole the academic models are inferior to the commercial ones.

Within in each class of model, commercial and academic, there is not a clear top model. However, we note that on the academic model side, MogFace significantly outperforms the other two models on every dataset except CCD. It is unknown as to why MogFace has such high performance, but we hypothesize a reason for what might explain this. MogFace was published very recently (late 2021), and perhaps much more recently than the commercial models. Only Azure indicates when its model was released (February 2021). The analysis of the commercial providers was also done prior to the release of MogFace. While more contemporary models do not necessarily imply better performance, this could be playing a role.

4.1.1 Performance of Individual Perturbations

Recall that there are four types of ImageNet-C corruptions: noise, blur, weather, and digital. On Adience, Brightness is the easiest corruption and noise is the hardest on five of the six models – GCP performs best on Pixelate and worst on Snow. On CCD, all models perform best on Glass Blur but worst on Zoom Blur.

Again, the zoom blur corruption proves particularly difficult on the MIAP datasets – it is the worst performer on all models for this dataset, whereas Brightness is the easiest on four of the six models. On UTKFace, elastic-transform is a notable corruption which the models struggle with – all models except TinaFace and Yolo5Face perform worst on elastic transform and UTKFace; all models except GCP perform best on Brightness. TinaFace and Yolo5Face struggle very significantly with the noise corruptions on UTKFace. Further details and analysis can be found in Table 1 and Appendix D.2.

4.2 RQ2: Demographic Disparities in Noise Robustness

We now turn our attention to answer RQ2: do face detection models have demographic disparities in their performance on noise robustness tasks? Each dataset we analyze has both perceived gender and perceived age labels and CCD has perceived skin type and lighting conditions.

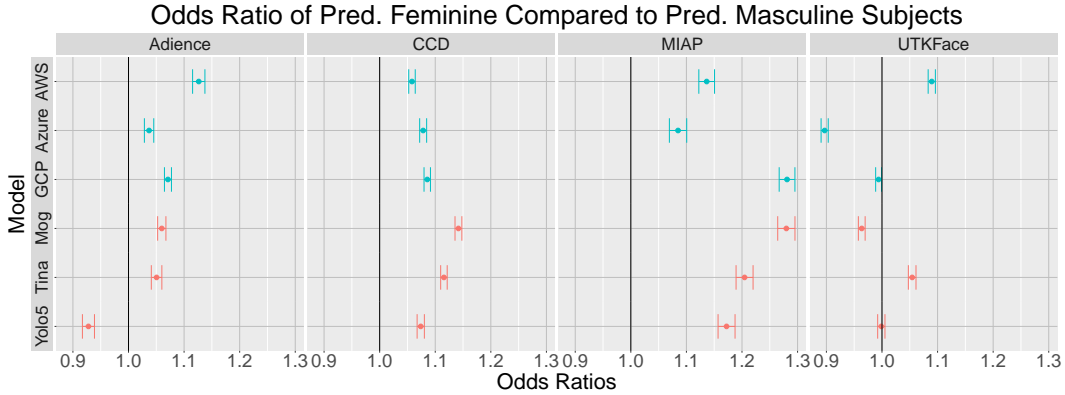


Figure 4: Gender disparity plots for each dataset and model. Values below 1 indicate that predominantly feminine presenting subjects are more susceptible to noise-induced changes. Values above 1 indicate that predominantly masculine presenting subjects are more susceptible to noise-induced changes. Error bars indicate 95% confidence.

4.2.1 Gender Disparities

We begin by first pausing to note that the labels we have for perceived gender were in all cases provided by a third-party human reviewer, and the labels fall within the gender binary. The one exception is the MIAP dataset which reports a category of “Unknown” for times when the human reviewers were unable to reach a decision on the perceived gender of the subject. While gender is not binary and gender identity is not something which third party reviewers can infer, we use the perceived gender concept in our work to measure how model performance may differ for people who present gender differently.

We visually depict the performance of each model on each dataset in Figure 4 broken down by perceived gender. We analyze the observed perceived gender disparities for each dataset separately with a report of the odds ratio of feminine presenting individuals over masculine presenting individuals. Recall, values over 1 indicate higher performance on those who are feminine presenting, and values less than 1 indicate higher performance on those who are masculine presenting.

We observe, qualitatively, across the 24 dataset and model combinations, there is a bias against masculine presenting individuals in 19 of them, there is a bias against feminine presenting subjects in 4, and there is no bias in one. This is a rather surprising result as previous reports indicate biases against feminine presenting individuals in facial recognition technology.

We further observe that the UTKFace dataset has the lowest robustness bias for perceived gender across all the models. This indicates that the dataset itself is an important tool in the measurement of algorithmic disparities and suggests that future work in this domain area should greatly expand their studies to incorporate multiple datasets.

4.2.2 Age Disparities

We move on to a discussion of the age disparities present in these models and datasets. We report the results of this age disparity in Figure 5. We note again, that age labels are given by perceived age of the subject in the image. Adience provides disparate age categories, MIAP provides age groupings (Young, Middle, Older, and Unknown) and UTKFace natively provides a numeric value. Since numeric age values from UTKFace are likely misspecified as it is nearly impossible to correctly predict a person’s age from a photo, we bin these numeric values into four buckets of (0-18), (19-45), (45-65) and (65+).

Qualitatively, looking at all these results, we observe that the oldest group always is more susceptible to noise-induced changes compared to middle aged individuals. Quantitatively as well, we see that the oldest group is always statistically significantly the lowest performer of the groups. We note that while there may be differences in the sample sizes of these groups, the statistical tests are robust to these differences and account for sample size differences. Statistical test results for Pairwise Wilcoxon Rank Sum Tests can be found in the Appendix.

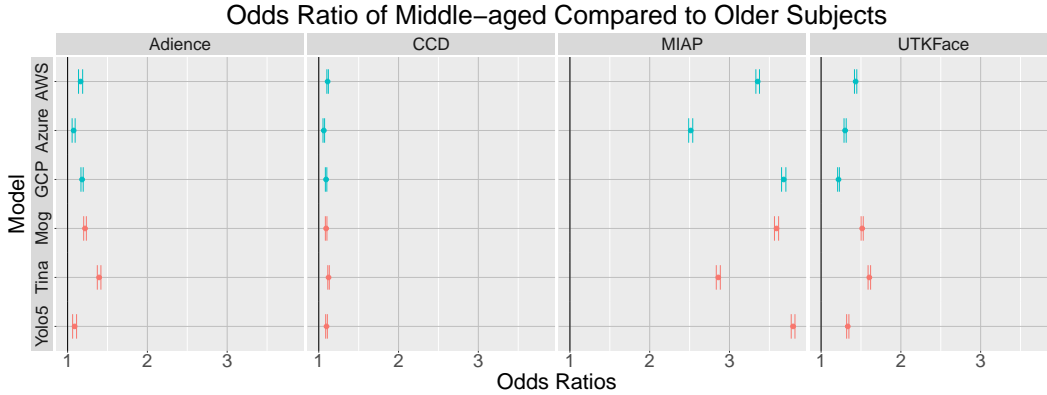


Figure 5: Age disparity plots for each dataset and model. Values greater than 1 indicate that older subjects are more susceptible to noise-induced changes compared to middle aged subjects. Error bars indicate 95% confidence.

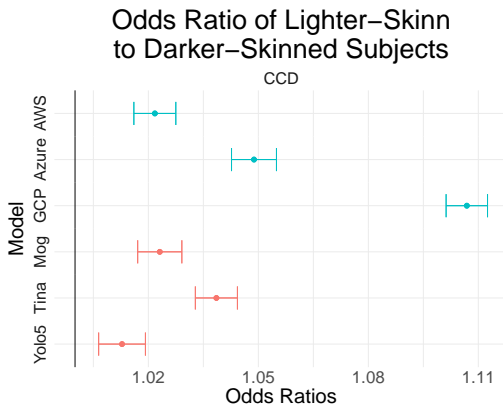


Figure 6: Skin type disparity plots for CCD. Values above 1 indicate that darker-skinned subjects are more susceptible to noise-induced changes. Error bars indicate 95% confidence.

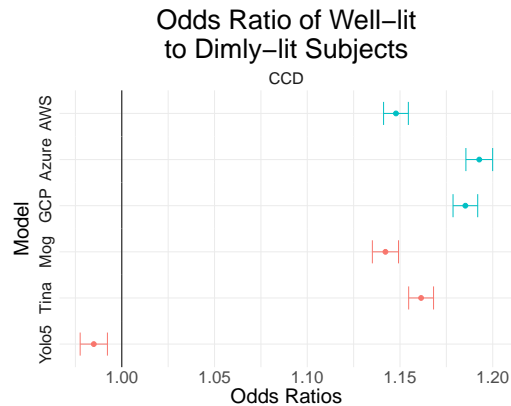


Figure 7: Lighting disparity plots for CCD. Values above 1 indicate that dimly-lit subjects are more susceptible to noise-induced changes. Error bars indicate 95% confidence.

For MIAP, we observe significantly higher biases against older individuals than we do for the other datasets. We hypothesize that this might be due to the way in which the MIAP dataset was collected and the nature of the more natural images of entire scenes with sometimes multiple faces in them.

4.2.3 Skin Type and Lighting Disparities

The only dataset which includes metadata on skin type and illumination is the CCD dataset. As was customary at the time of the dataset release, CCD reports annotator provided Fitzpatrick skin type labels which we split into two groups: Lighter (for ratings I-III) and Darker for ratings (IV-VI).

We observe a statistically significant bias against dark skinned individuals across every model, as can be seen in Figure 6. We further report that the bias between skin types is highest in the youngest groups; and this bias decreases in older groups. We also see a similar trend in the intersectional identities available in the CCD metadata (age, perceived gender, and skin type). We see that in every identity (except for 45-64 year old and Other gendered) the darker skin type has statistically significant lower AP. This difference is particularly stark in 19-45 year old, masculine subjects.

Lighting condition is also included as a metadata label in the CCD dataset. In Figure 7, we see that every model, except for YOLO5Face, exhibits behavior such that dimly lit images are more susceptible to noise-induced changes than brightly lit images. Interestingly and across the board, we generally see that the disparity in demographic groups decreases between bright and dimly lit environments. For example, the difference in precision between dark and light skinned subjects decreases to zero in dimly lit environments. This is also true for age groups. However, this is not true for individuals with gender presentations as Other or omitted.

4.3 RQ3: Disparity Comparison to Between Academic and Commercial Models

To answer RQ3, we examine the ordering and overlapping of the confidence intervals in the Figures 4-7. We note that we do not see signs of systemic differences between academic and commercial models in terms of their demographic disparities. When we examine the most biased model in each of the dataset and sociodemographic pairings, we observe no clear pattern. Commercial models are most biased in skin type and lighting variables as well as on Adience and UTKFace in the perceived gender variable. Academic models are most biased on the CCD dataset in the perceived gender variable as well as every dataset except for CCD on the age variable. (They are tied in the other two instances). Thus, we conclude there is no systematic difference in the magnitude of the disparity exhibited by commercial and academic models writ large.

5 Implications and Hypotheses

Above, we have shown striking disparities in commercial facial analysis systems. These biases have potential for real harms felt by individuals. Facial *detection* is the first step in facial recognition. As such, the biases which we report here will propagate downstream into further facial analysis systems. Facial detection bias is the starting point for bias in other facial analyses, and research that addresses biases in detection will also serve any other facial analysis system which uses its outputs. However, downstream systems will still have their own biases.

Since we are external researchers, we can only speculate as to why these disparities and biases are observed since we do not have access to the models themselves. The biases for dark-skinned individuals and dimly-lit subjects is unfortunately aligned with many prior works on the subject. Among the reasons for this include luminance and pixel intensity, which unfortunately have been codified as being discriminatory against darker skinned people in photography for decades [43].

On the other hand, the findings about older individuals and masculine-presenting individuals offer contrasting conclusions from existing work that audits facial analysis technologies. Regarding the finding the systems are more susceptible to noise-induced changes on masculine presenting subjects, we hypothesize that this might have to do with the size that a feminine-presenting subject's *head* takes up in an image. One gender presentation marker is hair and we hypothesize that the subject's entire head size might be a confounding factor in this bias phenomenon. We unfortunately do not have the data to test this hypothesis (since ground truth data for face detection includes just data on the face), but one could collect such data with sufficient ground truth.

6 Discussion & A Call to action

Revisiting our research questions, we come away with rather clear answers. We see that face detection models:

- (RQ1):** show that their robustness to noise could be improved significantly;
- (RQ2):** have significant perceived sociodemographic disparities in their performance on noise robustness tasks; and
- (RQ3):** show similar degrees of demographic bias across both academic and commercial models.

We believe that these results beget three main conclusions for different audiences who are interested in face detection systems and/or algorithmic bias. Our results suggest that commercial systems generally are no less biased on noise robustness than academic systems, for the types of noise corruptions we benchmarked. This is a rather striking result considering the resources large companies have at their disposal to tackle problems like demographic disparities in their products. Additionally, since demographic disparities in commercial products became a crucible following the publication of Buolamwini and Gebu [7] in 2018, these corporations have had ample time to address and work towards solutions to these issues. While these companies have to varying degrees acknowledged the need to equal out demographic disparities in their products, we cannot fully know what investment they have placed on these issues, and specifically on disparities in noise robustness. So at this time, we can merely speculate.

If these companies have committed vast resources to address the demographic disparities in their products, and specifically in noise robustness, then our results lead us to conclude that these investments have generally not paid off. We conclude this because we now know that within each dataset and for most commercial model, there is at least one academic model which is at most as

biased than it is. Further, since these academic models are published publicly with full source code and training procedures, we know that these models have not included any fairness constraints or considerations. Thus, if these companies *have* invested heavily in this problem, then we conclude that their investments have not paid off.

However, it is perhaps overly optimistic to think that corporations have invested in the mitigation of demographic bias in noise robustness — although we posit that this is not likely because many real-world use cases for facial analysis occur under imperfect “in-the-wild” conditions that would introduce various forms of natural noise. If in fact they have not done so, our results give a clear benchmark and goalpost for these corporations to improve. While in most cases, the commercial models are the most biased system, we should endeavor to expect that if these corporations plan to continue to publicly sell face detection software — a very socially and ethically provocative tool — that they should be investing in mitigating these biases and be able to do better than academic models which have no fairness considerations.

Our results add to the increasing body of research which finds various pernicious forms of demographic bias in facial recognition technologies. We provided strong evidence of the demographic biases present in face detection systems. We conclude that despite all the talk and publicity about concerns of demographic disparities in commercially provide products, large technology companies are no better at eliminating bias for noise robustness than academic models. Thus, we end this work with two broad calls to action:

To industry: This benchmark shows that the highly-resourced companies are no better than academic models at this robustness disparity in facial detection, a rather surprising comparison between where a trillion-dollar company could be—by spending a vanishing fraction of their liquid capital—and where it *should* be—where “should” is, admittedly, a value judgment, but a bipartisan one [6], and one gaining increasing traction in those firms’ own home country [62].

Our call to action, then, is as follows: pay attention to, work with, and fund academic research in unfairness in facial detection and noise, specifically natural and synthetic styles of noise. As our present work shows, academic models run hand-in-hand with—and, indeed, by some metrics beat—commercially deployed systems, and it would be of great benefit to further encourage unrestricted growth in that space, and to fertilize that growth with cross-boundary communication of techniques that have been tried internally at for-profit firms. Specific to our setting, both the present work and previous works [e.g., 7, 61] would benefit immensely from at least partial access to the internal workings of commercial systems, including dataset curation processes. Beyond simply measuring disparities, the natural next step is to hypothesize reasons for those disparities and then to, at least partially, mitigate them via new techniques. Indeed, as this paper shows, state-of-the-art academic models are arguably *beating* commercial models in some ways, so the value within this communication would flow both ways. Without a clear line of communication between academic and industrial researchers, this latter process is hampered.

To the public sector: The public sector provides a great service in both impacting the evolution of, and creating as well as enforcing the present state of social and legal norms. For example, in the United States, for our specific setting, the National Institute of Standards and Technology (NIST) Face Recognition Vendor Test (FRVT) has measured and monitored progress in both commercial and academic facial analysis systems. It has been run for at least the last two decades, and has been updated numerous times. Indeed, in a recent FRVT Update, NISTIR 8280 (2019), NIST brought demographic concerns into the forefront. NIST’s venerable FRVT has a history of incorporating natural noise into its barrage of tests; we would ask NIST, and analogous non-regulatory and standards-settings bodies in other countries, to consider updating their tests (e.g., FRVT) to include the cross section of bias and forms of noise. Our work motivates the need for monitoring in this area.

To the regulatory side, we are encouraged by and seek further acceptance of results publicized by both academics and industrial researchers. Washington State aims to set an example here with its recently enacted State Bill 6281, which states “if the results of . . . independent testing identify material unfair performance differences across subpopulations . . . then the processor must develop and implement a plan to address the identified performance differences” [55]. We believe that this benchmark meets this definition and hope the public sector has a robust enforcement mechanism for such legislation. We encourage other researchers to continue to audit existing commercial products, and believe our approach to compare commercial models to academic models enriches the scholarly and social discourse about facial recognition technology.

References

- [1] E. Adeli, Q. Zhao, A. Pfefferbaum, E. V. Sullivan, L. Fei-Fei, J. C. Niebles, and K. M. Pohl. Representation learning with statistical independence to mitigate bias. In *Proceedings of the IEEE/CVF Winter Conference on Applications of Computer Vision*, pages 2513–2523, 2021.
- [2] A. Agarwal, A. Beygelzimer, M. Dudik, J. Langford, and H. Wallach. A reductions approach to fair classification. In *Proceedings of the 35th International Conference on Machine Learning*, volume 80, pages 60–69, 2018. URL <http://proceedings.mlr.press/v80/agarwal18a.html>.
- [3] S. Barocas, M. Hardt, and A. Narayanan. *Fairness and Machine Learning*. fairmlbook.org, 2019. <http://www.fairmlbook.org>.
- [4] S. Benthall and B. D. Haynes. Racial categories in machine learning. In *Proceedings of the conference on fairness, accountability, and transparency*, pages 289–298, 2019.
- [5] A. Beutel, J. Chen, Z. Zhao, and E. H. Chi. Data decisions and theoretical implications when adversarially learning fair representations. *arXiv preprint arXiv:1707.00075*, 2017.
- [6] A. Beyea and M. Kebede. Maine’s facial recognition law shows bipartisan support for protecting privacy. *TechCrunch*, July. 20 2021. URL <https://techcrunch.com/2021/07/20/maines-facial-recognition-law-shows-bipartisan-support-for-protecting-privacy/>.
- [7] J. Buolamwini and T. Gebru. Gender shades: Intersectional accuracy disparities in commercial gender classification. In S. A. Friedler and C. Wilson, editors, *Proceedings of the 1st Conference on Fairness, Accountability and Transparency*, volume 81 of *Proceedings of Machine Learning Research*, pages 77–91. PMLR, 23–24 Feb 2018. URL <https://proceedings.mlr.press/v81/buolamwini18a.html>.
- [8] J. Buolamwini and T. Gebru. Gender shades: Intersectional accuracy disparities in commercial gender classification. In *Proceedings of the 1st Conference on Fairness, Accountability and Transparency*, volume 81, pages 77–91, 2018. URL <http://proceedings.mlr.press/v81/buolamwini18a.html>.
- [9] V. Cherepanova, M. Goldblum, H. Foley, S. Duan, J. P. Dickerson, G. Taylor, and T. Goldstein. Lowkey: leveraging adversarial attacks to protect social media users from facial recognition. In *International Conference on Learning Representations (ICLR)*, 2021.
- [10] A. Chouldechova and A. Roth. The frontiers of fairness in machine learning. *arXiv preprint arXiv:1810.08810*, 2018.
- [11] W. Derringer. A surveillance net blankets china’s cities, giving police vast powers. *The New York Times*, Dec. 17 2019. URL <https://www.nytimes.com/2019/12/17/technology/china-surveillance.html>.
- [12] E. Diana, W. Gill, M. Kearns, K. Kenthapadi, and A. Roth. Convergent algorithms for (relaxed) minimax fairness. *arXiv preprint arXiv:2011.03108*, 2020.
- [13] M. Donini, L. Oneto, S. Ben-David, J. Shawe-Taylor, and M. Pontil. Empirical risk minimization under fairness constraints. In *Proceedings of the 32nd International Conference on Neural Information Processing Systems, NIPS’18*, page 2796–2806, 2018.
- [14] S. Dooley, T. Goldstein, and J. P. Dickerson. Robustness disparities in commercial face detection. *arXiv preprint arXiv:2108.12508*, 2021.
- [15] S. Dooley, G. Z. Wei, T. Goldstein, and J. P. Dickerson. Are commercial face detection models as biased as academic models? *arXiv preprint arXiv:2201.10047*, 2022.
- [16] A. Dosovitskiy, L. Beyer, A. Kolesnikov, D. Weissenborn, X. Zhai, T. Unterthiner, M. Dehghani, M. Minderer, G. Heigold, S. Gelly, J. Uszkoreit, and N. Houlsby. An image is worth 16x16 words: Transformers for image recognition at scale, 2021.
- [17] P. Drozdzowski, C. Rathgeb, A. Dantcheva, N. Damer, and C. Busch. Demographic bias in biometrics: A survey on an emerging challenge. *IEEE Transactions on Technology and Society*, 1(2):89–103, 2020.
- [18] C. Dwork, M. Hardt, T. Pitassi, O. Reingold, and R. Zemel. Fairness through awareness. In *Proceedings of the 3rd Innovations in Theoretical Computer Science Conference, ITCS*

- '12, page 214–226, New York, NY, USA, 2012. Association for Computing Machinery. ISBN 9781450311151. doi:10.1145/2090236.2090255. URL <https://doi.org/10.1145/2090236.2090255>.
- [19] H. Edwards and A. J. Storkey. Censoring representations with an adversary. In *4th International Conference on Learning Representations, ICLR 2016, San Juan, Puerto Rico, May 2-4, 2016, Conference Track Proceedings*, 2016. URL <http://arxiv.org/abs/1511.05897>.
- [20] E. Eiding, R. Enbar, and T. Hassner. Age and gender estimation of unfiltered faces. *IEEE Transactions on Information Forensics and Security*, 9(12):2170–2179, 2014.
- [21] H. El Khiyari and H. Wechsler. Face verification subject to varying (age, ethnicity, and gender) demographics using deep learning. *Journal of Biometrics and Biostatistics*, 7(323):11, 2016.
- [22] M. Feldman, S. A. Friedler, J. Moeller, C. Scheidegger, and S. Venkatasubramanian. Certifying and removing disparate impact. In *Knowledge Discovery and Data Mining*, pages 259–268, 2015.
- [23] T. B. Fitzpatrick. The validity and practicality of sun-reactive skin types i through vi. *Archives of dermatology*, 124(6):869–871, 1988.
- [24] C. Garvie. *The perpetual line-up: Unregulated police face recognition in America*. Georgetown Law, Center on Privacy & Technology, 2016.
- [25] R. Girshick, J. Donahue, T. Darrell, and J. Malik. Rich feature hierarchies for accurate object detection and semantic segmentation, 2014.
- [26] N. Goel, M. Yaghini, and B. Faltings. Non-discriminatory machine learning through convex fairness criteria. *Proceedings of the AAAI Conference on Artificial Intelligence*, 32(1), 2018. URL <https://ojs.aaai.org/index.php/AAAI/article/view/11662>.
- [27] Google. How google uses pattern recognition to make sense of images. <https://policies.google.com/technologies/pattern-recognition?hl=en-US>, 2021. Accessed: 2021-06-07.
- [28] P. Grother, M. Ngan, and K. Hanaoka. *Face Recognition Vendor Test (FVRT): Part 3, Demographic Effects*. National Institute of Standards and Technology, 2019.
- [29] D. Gutman. King County Council bans use of facial recognition technology by Sheriff’s Office, other agencies. *The Seattle Times*, June 2021. URL <https://www.seattletimes.com/seattle-news/politics/king-county-council-bans-use-of-facial-recognition-technology-by-sheriffs-office-other-agencies/>.
- [30] F. Hamidi, M. K. Scheuerman, and S. M. Branham. Gender recognition or gender reductionism? the social implications of embedded gender recognition systems. In *Proceedings of the 2018 chi conference on human factors in computing systems*, pages 1–13, 2018.
- [31] A. Hanna, E. Denton, A. Smart, and J. Smith-Loud. Towards a critical race methodology in algorithmic fairness. In *Proceedings of the 2020 conference on fairness, accountability, and transparency*, pages 501–512, 2020.
- [32] M. Hardt, E. Price, E. Price, and N. Srebro. Equality of opportunity in supervised learning. In *Advances in Neural Information Processing Systems*, volume 29, pages 3315–3323, 2016. URL <https://proceedings.neurips.cc/paper/2016/file/9d2682367c3935defcb1f9e247a97c0d-Paper.pdf>.
- [33] W. Hartzog. The secretive company that might end privacy as we know it. *The New York Times*, Jan. 18 2020. URL <https://www.nytimes.com/2020/01/18/technology/clearview-privacy-facial-recognition.html>.
- [34] C. Hazirbas, J. Bitton, B. Dolhansky, J. Pan, A. Gordo, and C. C. Ferrer. Towards measuring fairness in ai: the casual conversations dataset. *arXiv preprint arXiv:2104.02821*, 2021.
- [35] D. Hendrycks and T. Dietterich. Benchmarking neural network robustness to common corruptions and perturbations. 2019.
- [36] H. Hosseini, B. Xiao, and R. Poovendran. Google’s cloud vision API is not robust to noise. In *2017 16th IEEE international conference on machine learning and applications (ICMLA)*, pages 101–105. IEEE, 2017.

- [37] G. Jain and S. Parsheera. 1.4 billion missing pieces? auditing the accuracy of facial processing tools on indian faces. *First Workshop on Ethical Considerations in Creative applications of Computer Vision*, 2021.
- [38] S. Jaiswal, K. Duggirala, A. Dash, and A. Mukherjee. Two-face: Adversarial audit of commercial face recognition systems. In *Proceedings of the International AAAI Conference on Web and Social Media*, volume 16, pages 381–392, 2022.
- [39] S. Kantayya. Coded bias, 2020. Feature-length documentary.
- [40] O. Keyes. The misgendering machines: Trans/hci implications of automatic gender recognition. *Proceedings of the ACM on human-computer interaction*, 2(CSCW):1–22, 2018.
- [41] B. F. Klare, M. J. Burge, J. C. Klontz, R. W. V. Bruegge, and A. K. Jain. Face recognition performance: Role of demographic information. *IEEE Transactions on Information Forensics and Security*, 7(6):1789–1801, 2012.
- [42] P. Lahoti, A. Beutel, J. Chen, K. Lee, F. Prost, N. Thain, X. Wang, and E. H. Chi. Fairness without demographics through adversarially reweighted learning. *arXiv preprint arXiv:2006.13114*, 2020.
- [43] S. Lewis. The racial bias built into photography. *The New York Times*, 25, 2019.
- [44] H. Li, Z. Lin, X. Shen, J. Brandt, and G. Hua. A convolutional neural network cascade for face detection. In *2015 IEEE Conference on Computer Vision and Pattern Recognition (CVPR)*, pages 5325–5334, 2015. doi:10.1109/CVPR.2015.7299170.
- [45] T.-Y. Lin, M. Maire, S. Belongie, J. Hays, P. Perona, D. Ramanan, P. Dollár, and C. L. Zitnick. Microsoft coco: Common objects in context. In *European conference on computer vision*, pages 740–755. Springer, 2014.
- [46] T.-Y. Lin, P. Dollár, R. Girshick, K. He, B. Hariharan, and S. Belongie. Feature pyramid networks for object detection. In *Proceedings of the IEEE Conference on Computer Vision and Pattern Recognition (CVPR)*, July 2017.
- [47] W. Liu, D. Anguelov, D. Erhan, C. Szegedy, S. Reed, C.-Y. Fu, and A. C. Berg. Ssd: Single shot multibox detector. *Lecture Notes in Computer Science*, page 21–37, 2016. ISSN 1611-3349. doi:10.1007/978-3-319-46448-0_2. URL http://dx.doi.org/10.1007/978-3-319-46448-0_2.
- [48] S. Lohr. Facial recognition is accurate, if you’re a white guy. *New York Times*, 9, 2018.
- [49] D. Madras, E. Creager, T. Pitassi, and R. S. Zemel. Learning adversarially fair and transferable representations. In *Proceedings of the 35th International Conference on Machine Learning, ICML 2018, Stockholmsmässan, Stockholm, Sweden, July 10-15, 2018*, volume 80 of *Proceedings of Machine Learning Research*, pages 3381–3390. PMLR, 2018. URL <http://proceedings.mlr.press/v80/madras18a.html>.
- [50] P. Majumdar, S. Mittal, R. Singh, and M. Vatsa. Unravelling the effect of image distortions for biased prediction of pre-trained face recognition models. In *Proceedings of the IEEE/CVF International Conference on Computer Vision*, pages 3786–3795, 2021.
- [51] J. Marson and B. Forrest. Armed low-cost drones, made by turkey, reshape battlefields and geopolitics. *The Wall Street Journal*, Jun 2021. URL <https://www.wsj.com/articles/armed-low-cost-drones-made-by-turkey-reshape-battlefields-and-geopolitics-11622727370>.
- [52] N. Martinez, M. Bertran, and G. Sapiro. Minimax pareto fairness: A multi objective perspective. In *Proceedings of the 37th International Conference on Machine Learning*, volume 119, pages 6755–6764, 2020. URL <http://proceedings.mlr.press/v119/martinez20a.html>.
- [53] S. Minaee, P. Luo, Z. Lin, and K. Bowyer. Going deeper into face detection: A survey, 2021.
- [54] V. Nanda, S. Dooley, S. Singla, S. Feizi, and J. P. Dickerson. Fairness through robustness: Investigating robustness disparity in deep learning. In *Proceedings of the 2021 ACM Conference on Fairness, Accountability, and Transparency*, pages 466–477, 2021.
- [55] S. of Washington 66th Legislature 2020 Regular Session. Senate bill 6281. 2020. URL <https://lawfilesexternal.leg.wa.gov/biennium/2019-20/Pdf/Bills/Senate%20Bills/6281.pdf?q=20220121184945>.

- [56] A. J. O’Toole, P. J. Phillips, X. An, and J. Dunlop. Demographic effects on estimates of automatic face recognition performance. *Image and Vision Computing*, 30(3):169–176, 2012.
- [57] M. Padala and S. Gujar. Fnncc: Achieving fairness through neural networks. In *Proceedings of the Twenty-Ninth International Joint Conference on Artificial Intelligence, IJCAI-20*, pages 2277–2283. International Joint Conferences on Artificial Intelligence Organization, 7 2020. doi:10.24963/ijcai.2020/315. URL <https://doi.org/10.24963/ijcai.2020/315>.
- [58] P. J. Phillips, W. T. Scruggs, A. J. O’Toole, P. J. Flynn, K. W. Bowyer, C. L. Schott, and M. Sharpe. Frvt 2006 and ice 2006 large-scale results. *National Institute of Standards and Technology, NISTIR*, 7408(1):1, 2007.
- [59] P. J. Phillips, J. R. Beveridge, B. A. Draper, G. Givens, A. J. O’Toole, D. S. Bolme, J. Dunlop, Y. M. Lui, H. Sahibzada, and S. Weimer. An introduction to the good, the bad, & the ugly face recognition challenge problem. In *2011 IEEE International Conference on Automatic Face & Gesture Recognition (FG)*, pages 346–353. IEEE, 2011.
- [60] N. Quadrianto, V. Sharmanska, and O. Thomas. Discovering fair representations in the data domain. In *IEEE Conference on Computer Vision and Pattern Recognition, CVPR 2019, Long Beach, CA, USA, June 16-20, 2019*, pages 8227–8236. Computer Vision Foundation / IEEE, 2019. doi:10.1109/CVPR.2019.00842. URL http://openaccess.thecvf.com/content_CVPR_2019/html/Quadrianto_Discovering_Fair_Representations_in_the_Data_Domain_CVPR_2019_paper.html.
- [61] I. D. Raji and J. Buolamwini. Actionable auditing: Investigating the impact of publicly naming biased performance results of commercial ai products. In *Proceedings of the 2019 AAAI/ACM Conference on AI, Ethics, and Society*, pages 429–435, 2019.
- [62] K. Ruane. Biden must halt face recognition technology to advance racial equity. *ACLU*, Feb. 17 2021. URL <https://www.aclu.org/news/privacy-technology/biden-must-halt-face-recognition-technology-to-advance-racial-equity/>.
- [63] H. J. Ryu, H. Adam, and M. Mitchell. Inclusivefacenet: Improving face attribute detection with race and gender diversity. *arXiv preprint arXiv:1712.00193*, 2018.
- [64] Y. Savani, C. White, and N. S. Govindarajulu. Intra-processing methods for debiasing neural networks. In *Proceedings of Advances in Neural Information Processing Systems*, 2020.
- [65] C. Schumann, C. R. Pantofaru, S. Ricco, U. Prabhu, and V. Ferrari. A step toward more inclusive people annotations for fairness. In *Proceedings of the AAAI/ACM Conference on AI, Ethics, and Society*, 2021.
- [66] S. Shan, E. Wenger, J. Zhang, H. Li, H. Zheng, and B. Y. Zhao. Fawkes: Protecting privacy against unauthorized deep learning models. In *29th {USENIX} Security Symposium ({USENIX} Security 20)*, pages 1589–1604, 2020.
- [67] N. Singer. Microsoft urges congress to regulate use of facial recognition. *The New York Times*, 2018.
- [68] R. Singh, A. Agarwal, M. Singh, S. Nagpal, and M. Vatsa. On the robustness of face recognition algorithms against attacks and bias. In *Proceedings of the AAAI Conference on Artificial Intelligence*, volume 34, pages 13583–13589, 2020.
- [69] R. Singh, P. Majumdar, S. Mittal, and M. Vatsa. Anatomizing bias in facial analysis. In *Proceedings of the AAAI Conference on Artificial Intelligence*, volume 36, pages 12351–12358, 2022.
- [70] A. Vaswani, N. Shazeer, N. Parmar, J. Uszkoreit, L. Jones, A. N. Gomez, L. u. Kaiser, and I. Polosukhin. Attention is all you need. In I. Guyon, U. V. Luxburg, S. Bengio, H. Wallach, R. Fergus, S. Vishwanathan, and R. Garnett, editors, *Advances in Neural Information Processing Systems*, volume 30. Curran Associates, Inc., 2017. URL <https://proceedings.neurips.cc/paper/2017/file/3f5ee243547dee91fbd053c1c4a845aa-Paper.pdf>.
- [71] M. Wang and W. Deng. Mitigating bias in face recognition using skewness-aware reinforcement learning. In *Proceedings of the IEEE/CVF Conference on Computer Vision and Pattern Recognition*, pages 9322–9331, 2020.
- [72] T. Wang, J. Zhao, M. Yatskar, K.-W. Chang, and V. Ordonez. Balanced datasets are not enough: Estimating and mitigating gender bias in deep image representations. In *Proceedings of the IEEE International Conference on Computer Vision*, pages 5310–5319, 2019.

- [73] Z. Wang, K. Qinami, I. C. Karakozis, K. Genova, P. Nair, K. Hata, and O. Russakovsky. Towards fairness in visual recognition: Effective strategies for bias mitigation, 2020.
- [74] K. Weise and N. Singer. Amazon pauses police use of its facial recognition software. *The New York Times*, Jul. 10 2020. URL <https://www.nytimes.com/2020/06/10/technology/amazon-facial-recognition-backlash.html>.
- [75] M. J. Wilber, V. Shmatikov, and S. Belongie. Can we still avoid automatic face detection? In *2016 IEEE Winter Conference on Applications of Computer Vision (WACV)*, pages 1–9. IEEE, 2016.
- [76] Y. Xiong, K. Zhu, D. Lin, and X. Tang. Recognize complex events from static images by fusing deep channels. In *Computer Vision and Pattern Recognition (CVPR), 2015 IEEE Conference on*. IEEE, 2015.
- [77] S. Yang, P. Luo, C. C. Loy, and X. Tang. Wider face: A face detection benchmark. In *IEEE Conference on Computer Vision and Pattern Recognition (CVPR)*, 2016.
- [78] M. B. Zafar, I. Valera, M. Gomez Rodriguez, and K. P. Gummadi. Fairness beyond disparate treatment & disparate impact. *Proceedings of the 26th International Conference on World Wide Web*, Apr 2017. doi:10.1145/3038912.3052660. URL <http://dx.doi.org/10.1145/3038912.3052660>.
- [79] M. B. Zafar, I. Valera, M. Gomez-Rodriguez, and K. P. Gummadi. Fairness constraints: Mechanisms for fair classification. In *Proceedings of the 20th International Conference on Artificial Intelligence and Statistics, AISTATS 2017, 20-22 April 2017, Fort Lauderdale, FL, USA*, volume 54 of *Proceedings of Machine Learning Research*, pages 962–970. PMLR, 2017. URL <http://proceedings.mlr.press/v54/zafar17a.html>.
- [80] M. B. Zafar, I. Valera, M. Gomez-Rodriguez, and K. P. Gummadi. Fairness constraints: A flexible approach for fair classification. *Journal of Machine Learning Research*, 20(75):1–42, 2019. URL <http://jmlr.org/papers/v20/18-262.html>.
- [81] R. Zemel, Y. Wu, K. Swersky, T. Pitassi, and C. Dwork. Learning fair representations. volume 28 of *Proceedings of Machine Learning Research*, pages 325–333, Atlanta, Georgia, USA, 17–19 Jun 2013. PMLR. URL <http://proceedings.mlr.press/v28/zemel13.html>.
- [82] Z. Zhang, Y. Song, and H. Qi. Age progression/regression by conditional adversarial autoencoder. In *Proceedings of the IEEE conference on computer vision and pattern recognition*, pages 5810–5818, 2017.

A Evaluation Information

A.1 Metrics

Precision. To evaluate the change that image corruptions have to face detection systems, we measure the precision of the corrupted images while using the detections from the clean image as ground truth. While this approach obviates the need for real ground truth bounding boxes, it is also a principled measurement strategy for our main research question. Since we are primarily interested in how the system is affected by the corruption, this metric is superior to using real ground truth bounding boxes. This follows because we’re interested in isolating the change in a system under a corruption which is exactly what this method measures.

To compute precision, we first observe the face detections on each clean image. After subsequently observing the face detection of a corrupted version of the clean image, we compute the image-level precision and recall for the corrupted image while using whatever the clean image’s detections were as ground truth.

A.2 Image Counts

For each dataset, we selected no more than 1,500 images from any intersectional group. The final tallies of how many images from each group can be found in Tables 2, 3, 4, and 5.

A.3 Corruption information

We evaluate 15 corruptions from Hendrycks and Dietterich [35]: Gaussian noise, shot noise, impulse noise, defocus blur, glass blur, motion blur, zoom blur, snow, frost, fog, brightness, contrast, elastic transforms, pixelation, and jpeg compressions. Each corruption is described in the Hendrycks and Dietterich [35] paper as follows:

The first corruption type is Gaussian noise. This corruption can appear in low-lighting conditions. Shot noise, also called Poisson noise, is electronic noise caused by the discrete nature of light itself. Impulse noise is a color analogue of salt-and-pepper noise and can be caused by bit errors. Defocus blur occurs when an image is out of focus. Frosted Glass Blur appears with “frosted glass” windows or panels. Motion blur appears when a camera is moving quickly. Zoom blur occurs when a camera moves toward an object rapidly. Snow is a visually obstructive form of precipitation. Frost forms when lenses or windows are coated with ice crystals. Fog shrouds objects and is rendered with the diamond-square algorithm. Brightness varies with daylight intensity. Contrast can be high or low depending on lighting conditions and the photographed object’s color. Elastic transformations stretch or contract small image regions. Pixelation occurs when upsampling a lowresolution image. JPEG is a lossy image compression format which introduces compression artifacts.

The specific parameters for each corruption can be found in the project’s github at the corruptions file: https://github.com/dooleys/Robustness-Disparities-in-Commercial-Face-Detection/blob/main/code/imagenet_c_big/corruptions.py.

B API Parameters

For the AWS DetectFaces API,² we selected to have all facial attributes returned. The Azure Face API³ allows the user to select one of three detection models. We chose model `detection_03` as it was their most recently released model (February 2021) and was described to have the highest performance on small, side, and blurry faces, since it aligns with our benchmark intention. This model does not return age or gender estimates (though model `detection_01` does).

These experiments were conducted in July 2021.

C Benchmarks Costs

A total breakdown of costs for this benchmark can be found in Table 6.

²https://docs.aws.amazon.com/rekognition/latest/dg/API_DetectFaces.html

³<https://westus.dev.cognitive.microsoft.com/docs/services/563879b61984550e40cbbe8d/operations/563879b61984550f30395236>

Table 1: The best and worst performing perturbations for each dataset and model.

		AWS	Azure	GCP	MogFace	TinaFace	Yolo5Face
Adience	Best	Brightness	Brightness	Pixelate	Brightness	Brightness	Brightness
	Worst	Impulse Noise	Shot Noise	Snow	Impulse Noise	Impulse Noise	Impulse Noise
CCD	Best	Glass Blur	Glass Blur	Glass Blur	Glass Blur	Glass Blur	Glass Blur
	Worst	Zoom Blur	Zoom Blur	Zoom Blur	Zoom Blur	Zoom Blur	Zoom Blur
MIAP	Best	Brightness	Glass Blur	JPEG Compression	Brightness	Brightness	Brightness
	Worst	Zoom Blur	Zoom Blur	Zoom Blur	Zoom Blur	Zoom Blur	Zoom Blur
UTKFace	Best	Brightness	Brightness	JPEG Compression	Brightness	Brightness	Brightness
	Worst	Elastic Transform	Elastic Transform	Elastic Transform	Elastic Transform	Impulse Noise	Shot Noise

Table 2: Adience Dataset Counts

Age	Gender	Count
0-2	Female	684
	Male	716
3-7	Female	1232
	Male	925
8-14	Female	1353
	Male	933
15-24	Female	1047
	Male	742
25-35	Female	1500
	Male	1500
36-45	Female	1078
	Male	1412
46-59	Female	436
	Male	466
60+	Female	428
	Male	467

D Statistical Significance Regressions for Average Precision

D.1 Main Tables

AP p -values for pairwise Wilcoxon test with Bonferroni correction for model on the Adience dataset can be found in Table 7

AP p -values for pairwise Wilcoxon test with Bonferroni correction for model on the CCD dataset can be found in Table 8

AP p -values for pairwise Wilcoxon test with Bonferroni correction for model on the MIAP dataset can be found in Table 9

AP p -values for pairwise Wilcoxon test with Bonferroni correction for model on the UTK dataset can be found in Table 10

D.2 AP — Corruption Comparison Claims

AP p -values for pairwise Wilcoxon test with Bonferroni correction for corruption on AWS and Adience can be found in Table 11

Table 3: CCD Dataset Counts

Lighting	Gender	Skin	Age	Count
Bright	Female	Dark	19-45	1500
			45-64	1500
			65+	547
		Light	19-45	1500
			45-64	1500
			65+	653
	Male	Dark	19-45	1500
			45-64	1500
			65+	384
		Light	19-45	1500
			45-64	1500
			65+	695
Other	Dark	19-45	368	
		45-64	168	
		65+	12	
	Light	19-45	244	
		45-64	49	
Dim	Female	Dark	19-45	1500
			45-64	670
			65+	100
		Light	19-45	642
			45-64	314
			65+	131
	Male	Dark	19-45	1500
			45-64	387
			65+	48
		Light	19-45	485
			45-64	299
			65+	123
Other	Dark	19-45	57	
		45-64	26	
		65+	3	
	Light	19-45	27	
		45-64	12	

Table 4: MIAP Dataset Counts

AgePresentation	GenderPresentation	Count
Young	Unknown	1500
Middle	Predominantly Feminine	1500
	Predominantly Masculine	1500
	Unknown	561
Older	Predominantly Feminine	209
	Predominantly Masculine	748
	Unknown	24
Unknown	Predominantly Feminine	250
	Predominantly Masculine	402
	Unknown	1500

Table 5: UTKFace Dataset Counts

Age	Gender	Race	Count
0-18	Female	Asian	555
		Black	161
		Indian	350
		Others	338
		White	987
	Male	Asian	586
		Black	129
		Indian	277
		Others	189
		White	955
19-45	Female	Asian	1273
		Black	1500
		Indian	1203
		Others	575
		White	1500
	Male	Asian	730
		Black	1499
		Indian	1264
		Others	477
		White	1500
45-64	Female	Asian	39
		Black	206
		Indian	146
		Others	22
		White	802
	Male	Asian	180
		Black	401
		Indian	653
		Others	97
		White	1500
65+	Female	Asian	75
		Black	78
		Indian	43
		Others	10
		White	712
	Male	Asian	148
		Black	166
		Indian	91
		Others	5
		White	682

Table 6: Total Costs of Benchmark

Category	Cost
Azure Face Service	\$4,270.58
AWS Rekognition	\$4,270.66
Google Cloud Platform	\$7,230.47
S3	\$1,003.83
EC2	\$475.77
Tax	\$256.24
Total	\$17,507.55

Table 7: AP. Pairwise Wilcoxon test with Bonferroni correction for model on Adience

	AWS	Azure	GCP	MogFace	TinaFace
Azure	0				
GCP	0	0			
MogFace	0	0	0		
TinaFace	0	0	0	0	
Yolov5	0	0	0	0	0

Table 8: AP. Pairwise Wilcoxon test with Bonferroni correction for model on CCD

	AWS	Azure	GCP	MogFace	TinaFace
Azure	0				
GCP	0	0			
MogFace	0	0.071	0		
TinaFace	0	0	0	0	
Yolov5	0	0	0	0	0

Table 9: AP. Pairwise Wilcoxon test with Bonferroni correction for model on MIAP

	AWS	Azure	GCP	MogFace	TinaFace
Azure	0				
GCP	0	0			
MogFace	0	0	0		
TinaFace	0	0	0	0	
Yolov5	0	0	0	0	0

Table 10: AP. Pairwise Wilcoxon test with Bonferroni correction for model on UTK

	AWS	Azure	GCP	MogFace	TinaFace
Azure	0				
GCP	0	0			
MogFace	0	0	0		
TinaFace	0	0	0	0	
Yolov5	0	0	0	0	0

Table 11: AP. Pairwise Wilcoxon test with Bonferroni correction for corruption on AWS and Adience

	gaussian-noise	shot-noise	impulse-noise	defocus-blur	glass-blur	motion-blur	zoom-blur	snow	frost	fog	brightness	contrast	elastic-transform	pixelate
shot-noise	0.099													
impulse-noise	0	0												
defocus-blur	0	0	0											
glass-blur	0	0	0	0										
motion-blur	0	0	0	0	0.779									
zoom-blur	0	0	0	0	0	0								
snow	0	0	0	0	0	0	0							
frost	0	0	0	0	0	0	0	0						
fog	0	0	0	0	0	0	0	0	0					
brightness	0	0	0	0	0	0	0	0	0	0				
contrast	0	0	0	0	0	0	0	0	0	0	0			
elastic-transform	0	0	0	0	0	0	0	0	0	0	0	0		
pixelate	0	0	0	0	0	0	0	0	0	0	0	0	0	
jpeg-compression	0	0	0	0	0	0	0.00000	0	0	0	0	0	0	0

AP p -values for pairwise Wilcoxon test with Bonferroni correction for corruption on Azure and Adience can be found in Table 12

Table 12: AP. Pairwise Wilcoxon test with Bonferroni correction for corruption on Azure and Adience

	gaussian-noise	shot-noise	impulse-noise	defocus-blur	glass-blur	motion-blur	zoom-blur	snow	frost	fog	brightness	contrast	elastic-transform	pixelate
shot-noise	0													
impulse-noise	0.958	0												
defocus-blur	0	0	0											
glass-blur	0	0	0	0										
motion-blur	0	0	0	0	0									
zoom-blur	0	0	0	0	0	0								
snow	0	0	0	0	0	0	0							
frost	0	0	0	0	0	0	0	0.0003						
fog	0	0	0	0.008	0	0	0	0	0					
brightness	0	0	0	0	0	0	0	0	0	0				
contrast	0	0	0	0	0	0	0	0	0	0	0			
elastic-transform	0	0	0	0	0	0	0	0	0	0	0	0		
pixelate	0	0	0	0	0	0	0	0	0	0	0	0	0	
jpeg-compression	0	0	0	0	0	0	0	0	0	0	0	0	0	0

AP p -values for pairwise Wilcoxon test with Bonferroni correction for corruption on GCP and Adience can be found in Table 13

Table 13: AP. Pairwise Wilcoxon test with Bonferroni correction for corruption on GCP and Adience

	gaussian-noise	shot-noise	impulse-noise	defocus-blur	glass-blur	motion-blur	zoom-blur	snow	frost	fog	brightness	contrast	elastic-transform	pixelate
shot-noise	0													
impulse-noise	0	0.0005												
defocus-blur	0	0	0											
glass-blur	0	0	0	0										
motion-blur	0.278	0	0	0	0									
zoom-blur	0	0	0	0	0	0								
snow	0	0	0	0	0	0	0							
frost	0	0	0	0	0	0	0	0						
fog	0	0	0	0	0	0	0	0	0					
brightness	0	0	0	0	0	0	0	0	0	0				
contrast	0	0	0	0	0	0	0	0	0	0	0			
elastic-transform	0	0	0	0	0	0	0	0	0	0	0	0		
pixelate	0	0	0	0	0	0	0	0	0	0	0	0	0	
jpeg-compression	0	0	0	0	0	0	0	0	0	0	0	0	0	0

AP p -values for pairwise Wilcoxon test with Bonferroni correction for corruption on MogFace and Adience can be found in Table 14

Table 14: AP. Pairwise Wilcoxon test with Bonferroni correction for corruption on MogFace and Adience

	gaussian-noise	shot-noise	impulse-noise	defocus-blur	glass-blur	motion-blur	zoom-blur	snow	frost	fog	brightness	contrast	elastic-transform	pixelate
shot-noise	0													
impulse-noise	0	0												
defocus-blur	0	0	0											
glass-blur	0	0	0	0										
motion-blur	0	0	0	0	0									
zoom-blur	0	0	0	0	0	0								
snow	0.0001	0	0	0	0	0	0							
frost	0	0	0	0	0	0	0	0						
fog	0	0	0	0	0	0	0	0	0					
brightness	0	0	0	0	0	0	0	0	0	0				
contrast	0	0	0	0	0	0	0	0	0	0.120	0			
elastic-transform	0	0	0	0	0	0	0.034	0	0	0	0	0		
pixelate	0	0	0	0	0	0	0	0	0	0	0	0	0	
jpeg-compression	0	0	0	0	0	0	0	0	0	0	0	0	0	0

AP p -values for pairwise Wilcoxon test with Bonferroni correction for corruption on TinaFace and Adience can be found in Table 15

AP p -values for pairwise Wilcoxon test with Bonferroni correction for corruption on Yolov5 and Adience can be found in Table 16

AP p -values for pairwise Wilcoxon test with Bonferroni correction for corruption on AWS and CCD can be found in Table 17

Table 15: AP. Pairwise Wilcox test with Bonferroni correction for corruption on TinaFace and Adience

	gaussian-noise	shot-noise	impulse-noise	defocus-blur	glass-blur	motion-blur	zoom-blur	snow	frost	fog	brightness	contrast	elastic-transform	pixelate
shot-noise	0.0001													
impulse-noise	0	0												
defocus-blur	0	0	0											
glass-blur	0	0	0	0										
motion-blur	0	0	0	0	0									
zoom-blur	0	0	0	0	0	0								
snow	0	0	0	0	0	0	0							
frost	0	0	0	0	0	0	0	0						
fog	0	0	0	0	0	0	0	0	0					
brightness	0	0	0	0	0	0	0	0	0	0				
contrast	0	0	0	0	0	0	0	0	0	0	0			
elastic-transform	0	0	0	0	0	0	0	0	0	0	0	0		
pixelate	0	0	0	0	0	0	0	0	0	0.0001	0	0	0	
jpeg-compression	0	0	0	0	0	0.047	0	0	0	0	0	0	0	0

Table 16: AP. Pairwise Wilcox test with Bonferroni correction for corruption on Yolov5 and Adience

	gaussian-noise	shot-noise	impulse-noise	defocus-blur	glass-blur	motion-blur	zoom-blur	snow	frost	fog	brightness	contrast	elastic-transform	pixelate
shot-noise	0.004													
impulse-noise	0	0.00000												
defocus-blur	0	0	0											
glass-blur	0	0	0	0.005										
motion-blur	0	0	0	0	0									
zoom-blur	0	0	0	0	0	0								
snow	0	0	0	0	0	0	0							
frost	0	0	0	0	0	0	0	0						
fog	0	0	0	0	0	0	0	0	0					
brightness	0	0	0	0	0	0	0	0	0	0				
contrast	0	0	0	0	0	0	0	0.00000	0	0				
elastic-transform	0	0	0	0	0	0	0	0	0	0	0.643			
pixelate	0	0	0	0	0	0	0	0	0	0	0	0	0	
jpeg-compression	0	0	0	0	0	0	0	0	0	0	0	0	0	0

Table 17: AP. Pairwise Wilcox test with Bonferroni correction for corruption on AWS and CCD

	gaussian-noise	shot-noise	impulse-noise	defocus-blur	glass-blur	motion-blur	zoom-blur	snow	frost	fog	brightness	contrast	elastic-transform	pixelate
shot-noise	0													
impulse-noise	0	0												
defocus-blur	0	0	0											
glass-blur	0	0	0	0										
motion-blur	0	0	0	0	0									
zoom-blur	0	0	0	0	0	0								
snow	0	0	0	0	0	0	0							
frost	0	0	0	0	0	0	0	0						
fog	0	0	0	0	0	0	0	0	0					
brightness	0	0	0	0	0	0	0	0	0	0				
contrast	0	0	0	0	0	0	0	0	0	0	0			
elastic-transform	0	0	0	0	0	0	0	0	0	0	0	0		
pixelate	0	0	0	0	0	0	0	0	0	0	0	0	0	
jpeg-compression	0	0	0	0	0	0	0	0	0	0	0	0	0	0.0001

AP p -values for pairwise Wilcox test with Bonferroni correction for corruption on Azure and CCD can be found in Table 18

Table 18: AP. Pairwise Wilcox test with Bonferroni correction for corruption on Azure and CCD

	gaussian-noise	shot-noise	impulse-noise	defocus-blur	glass-blur	motion-blur	zoom-blur	snow	frost	fog	brightness	contrast	elastic-transform	pixelate
shot-noise	0													
impulse-noise	0	0												
defocus-blur	0	0	0											
glass-blur	0	0	0	0										
motion-blur	0	0	0	0	0									
zoom-blur	0	0	0	0	0	0								
snow	0	0	0	0	0	0	0							
frost	0	0	0	0	0	0	0	0						
fog	0	0	0	0.00000	0	0	0	0	0					
brightness	0	0	0	0	0	0	0	0	0	0				
contrast	0	0	0	0	0	0	0	0	0	0	0			
elastic-transform	0	0	0	0	0	0	0	0	0	0	0	0		
pixelate	0	0	0	0	0	0	0	0	0	0	0	0	0	
jpeg-compression	0	0	0	0	0	0	0	0	0	0	0	0	0	0

AP p -values for pairwise Wilcox test with Bonferroni correction for corruption on GCP and CCD can be found in Table 19

Table 19: AP. Pairwise Wilcox test with Bonferroni correction for corruption on GCP and CCD

	gaussian-noise	shot-noise	impulse-noise	defocus-blur	glass-blur	motion-blur	zoom-blur	snow	frost	fog	brightness	contrast	elastic-transform	pixelate
shot-noise	0													
impulse-noise	0.00000	0												
defocus-blur	0	0	0											
glass-blur	0	0	0	0										
motion-blur	0	0	0	0	0									
zoom-blur	0	0	0	0	0	0								
snow	0	0	0	0	0	0	0							
frost	0	0	0	0	0	0	0	0						
fog	0	0	0	0	0	0	0	0	0					
brightness	0	0	0	0	0	0	0	0	0	0				
contrast	0	0	0	0	0	0	0	0	0	0	0			
elastic-transform	0	0	0	0	0	0	0	0	0	0	0	0		
pixelate	0	0	0	0	0	0	0	0	0	0	0	0	0	
jpeg-compression	0	0	0	0	0	0	0	0	0	0	0	0	0	0

AP p -values for pairwise Wilcoxon test with Bonferroni correction for corruption on MogFace and CCD can be found in Table 20

Table 20: AP. Pairwise Wilcoxon test with Bonferroni correction for corruption on MogFace and CCD

	gaussian-noise	shot-noise	impulse-noise	defocus-blur	glass-blur	motion-blur	zoom-blur	snow	frost	fog	brightness	contrast	elastic-transform	pixelate
shot-noise	0													
impulse-noise	0	0												
defocus-blur	0	0	0											
glass-blur	0	0	0	0										
motion-blur	0	0	0	0	0									
zoom-blur	0	0	0	0	0	0								
snow	0	0	0	0	0	0	0							
frost	0	0	0	0	0	0	0	0						
fog	0	0	0	0	0	0	0	0	0					
brightness	0	0	0	0	0	0	0	0	0	0				
contrast	0	0	0	0	0	0	0	0	0	0	0			
elastic-transform	0	0	0	0	0	0	0	0	0	0	0	0		
pixelate	0	0	0	0	0	0	0	0	0	0.012	0	0	0	
jpeg-compression	0	0	0	0	0	0	0	0	0	0	0	0	0	0

AP p -values for pairwise Wilcoxon test with Bonferroni correction for corruption on TinaFace and CCD can be found in Table 21

Table 21: AP. Pairwise Wilcoxon test with Bonferroni correction for corruption on TinaFace and CCD

	gaussian-noise	shot-noise	impulse-noise	defocus-blur	glass-blur	motion-blur	zoom-blur	snow	frost	fog	brightness	contrast	elastic-transform	pixelate
shot-noise	0													
impulse-noise	0.00000	0												
defocus-blur	0	0	0											
glass-blur	0	0	0	0										
motion-blur	0.016	0	0.065	0	0									
zoom-blur	0	0	0	0	0	0								
snow	0	0	0	0	0	0	0							
frost	0	0	0	0	0	0	0	0						
fog	0	0	0	0	0	0	0	0	0					
brightness	0	0	0	0	0	0	0	0	0	0				
contrast	0	0	0	0	0	0	0	0	0	0	0			
elastic-transform	0	0	0	0	0	0	0	0	0	0	0	0		
pixelate	0	0	0	0	0	0	0	0	0	0	0	0	0	
jpeg-compression	0	0	0	0	0	0	0	0	0	0	0	0	0	0.0000

AP p -values for pairwise Wilcoxon test with Bonferroni correction for corruption on Yolov5 and CCD can be found in Table 22

Table 22: AP. Pairwise Wilcoxon test with Bonferroni correction for corruption on Yolov5 and CCD

	gaussian-noise	shot-noise	impulse-noise	defocus-blur	glass-blur	motion-blur	zoom-blur	snow	frost	fog	brightness	contrast	elastic-transform	pixelate
shot-noise	0													
impulse-noise	0	0												
defocus-blur	0	0	0											
glass-blur	0	0	0	0										
motion-blur	0	0	0	0	0									
zoom-blur	0	0	0	0	0	0								
snow	0	0	0	0	0	0	0							
frost	0	0	0	0	0	0	0	0						
fog	0	0	0	0	0	0	0	0	0					
brightness	0	0	0	0	0	0	0	0	0	0				
contrast	0	0	0	0	0	0	0	0	0	0	0			
elastic-transform	0	0	0	0	0	0	0	0	0	0	0	0		
pixelate	0	0	0	0	0	0	0	0	0	0	0	0	0	
jpeg-compression	0	0	0	0	0	0	0	0	0	0	0	0	0	0.822

AP p -values for pairwise Wilcoxon test with Bonferroni correction for corruption on AWS and MIAP can be found in Table 23

Table 23: AP. Pairwise Wilcoxon test with Bonferroni correction for corruption on AWS and MIAP

	gaussian-noise	shot-noise	impulse-noise	defocus-blur	glass-blur	motion-blur	zoom-blur	snow	frost	fog	brightness	contrast	elastic-transform	pixelate
shot-noise	0.018													
impulse-noise	0	0												
defocus-blur	0	0	0											
glass-blur	0	0	0	0										
motion-blur	0	0	0	0	0									
zoom-blur	0	0	0	0	0	0								
snow	0	0	0	0	0	0	0							
frost	0	0	0	0	0	0.00000	0	0						
fog	0	0	0	0	0	0	0	0	0					
brightness	0	0	0	0	0	0	0	0	0	0				
contrast	0	0	0	0	0	0	0	0	0	0	0			
elastic-transform	0	0	0	0	0	0	0	0	0	0	0	0		
pixelate	0	0	0	0	0	0	0	0	0	0	0	0	0	
jpeg-compression	0	0	0	0	0	0	0	0	0	0.009	0	0	0	0

AP p -values for pairwise Wilcoxon test with Bonferroni correction for corruption on Azure and MIAP can be found in Table 24

AP p -values for pairwise Wilcoxon test with Bonferroni correction for corruption on GCP and MIAP can be found in Table 25

Table 24: AP. Pairwise Wilcox test with Bonferroni correction for corruption on Azure and MIAP

	gaussian-noise	shot-noise	impulse-noise	defocus-blur	glass-blur	motion-blur	zoom-blur	snow	frost	fog	brightness	contrast	elastic-transform	pixelate
shot-noise	0.211													
impulse-noise	0.913	0.170												
defocus-blur	0	0	0											
glass-blur	0	0	0	0										
motion-blur	0	0	0	0	0									
zoom-blur	0	0	0	0	0	0								
snow	0	0	0	0	0	0	0							
frost	0	0	0	0	0	0.001	0	0.00000						
fog	0	0	0	0	0	0	0	0	0					
brightness	0	0	0	0	0	0	0	0	0	0				
contrast	0	0	0	0	0	0	0	0	0	0	0			
elastic-transform	0.203	0.730	0.061	0	0	0	0	0	0	0	0	0		
pixelate	0	0	0	0	0	0	0	0	0	0	0	0	0	
jpeg-compression	0	0	0	0	0	0	0	0	0	0	0	0	0	0.068

Table 25: AP. Pairwise Wilcox test with Bonferroni correction for corruption on GCP and MIAP

	gaussian-noise	shot-noise	impulse-noise	defocus-blur	glass-blur	motion-blur	zoom-blur	snow	frost	fog	brightness	contrast	elastic-transform	pixelate
shot-noise	0.123													
impulse-noise	0.131	0.963												
defocus-blur	0	0	0											
glass-blur	0	0	0	0										
motion-blur	0.018	0.450	0.309	0	0									
zoom-blur	0	0	0	0	0	0								
snow	0	0	0	0	0	0	0							
frost	0	0	0	0	0	0	0	0.006						
fog	0	0	0	0	0	0	0	0	0					
brightness	0	0	0	0	0	0	0	0	0	0				
contrast	0	0	0	0	0	0	0	0.001	0	0	0			
elastic-transform	0	0	0	0	0	0	0	0	0	0	0	0		
pixelate	0	0	0	0	0	0	0	0	0	0	0	0	0	
jpeg-compression	0	0	0	0	0.492	0	0	0	0	0	0	0	0	0

AP p -values for pairwise Wilcox test with Bonferroni correction for corruption on MogFace and MIAP can be found in Table 26

Table 26: AP. Pairwise Wilcox test with Bonferroni correction for corruption on MogFace and MIAP

	gaussian-noise	shot-noise	impulse-noise	defocus-blur	glass-blur	motion-blur	zoom-blur	snow	frost	fog	brightness	contrast	elastic-transform	pixelate
shot-noise	0.247													
impulse-noise	0.024	0.001												
defocus-blur	0	0	0											
glass-blur	0	0	0	0										
motion-blur	0	0	0	0	0									
zoom-blur	0	0	0	0	0	0								
snow	0	0	0	0	0	0	0							
frost	0	0	0	0	0	0	0	0						
fog	0	0	0	0	0	0	0	0	0					
brightness	0	0	0	0	0	0	0	0	0	0				
contrast	0	0	0	0	0	0	0	0	0	0	0			
elastic-transform	0	0	0	0	0	0	0	0	0	0	0	0		
pixelate	0	0	0	0	0	0	0	0	0	0	0	0	0	
jpeg-compression	0	0	0	0	0	0	0	0	0	0.575	0	0	0	0

AP p -values for pairwise Wilcox test with Bonferroni correction for corruption on TinaFace and MIAP can be found in Table 27

Table 27: AP. Pairwise Wilcox test with Bonferroni correction for corruption on TinaFace and MIAP

	gaussian-noise	shot-noise	impulse-noise	defocus-blur	glass-blur	motion-blur	zoom-blur	snow	frost	fog	brightness	contrast	elastic-transform	pixelate
shot-noise	0.571													
impulse-noise	0	0												
defocus-blur	0	0	0											
glass-blur	0	0	0	0										
motion-blur	0	0	0	0	0									
zoom-blur	0	0	0	0	0	0								
snow	0	0	0	0	0	0	0							
frost	0	0	0	0	0	0.215	0	0						
fog	0	0	0	0	0	0	0	0	0					
brightness	0	0	0	0	0	0	0	0	0	0				
contrast	0	0	0	0	0	0	0	0	0	0	0			
elastic-transform	0	0	0	0	0	0	0	0	0	0	0	0		
pixelate	0	0	0	0.0004	0	0	0	0	0	0	0	0	0	
jpeg-compression	0	0	0	0	0	0	0	0	0	0	0	0	0	0

AP p -values for pairwise Wilcox test with Bonferroni correction for corruption on Yolov5 and MIAP can be found in Table 28

AP p -values for pairwise Wilcox test with Bonferroni correction for corruption on AWS and UTK can be found in Table 29

AP p -values for pairwise Wilcox test with Bonferroni correction for corruption on Azure and UTK can be found in Table 30

AP p -values for pairwise Wilcox test with Bonferroni correction for corruption on GCP and UTK can be found in Table 31

Table 28: AP. Pairwise Wilcox test with Bonferroni correction for corruption on Yolov5 and MIAP

	gaussian-noise	shot-noise	impulse-noise	defocus-blur	glass-blur	motion-blur	zoom-blur	snow	frost	fog	brightness	contrast	elastic-transform	pixelate
shot-noise	0.002													
impulse-noise	0.00000	0												
defocus-blur	0	0	0											
glass-blur	0	0	0	0										
motion-blur	0	0	0	0	0									
zoom-blur	0	0	0	0	0	0								
snow	0	0	0	0	0	0	0							
frost	0	0	0	0	0	0	0	0						
fog	0	0	0	0	0	0	0	0	0					
brightness	0	0	0	0	0.013	0	0	0	0	0				
contrast	0	0	0	0	0	0	0	0	0.00003	0	0			
elastic-transform	0.014	0	0.007	0	0	0	0	0	0	0	0	0		
pixelate	0	0	0	0	0	0	0	0	0	0.014	0	0	0	
jpeg-compression	0	0	0	0	0	0	0	0	0	0	0	0	0	0

Table 29: AP. Pairwise Wilcox test with Bonferroni correction for corruption on AWS and UTK

	gaussian-noise	shot-noise	impulse-noise	defocus-blur	glass-blur	motion-blur	zoom-blur	snow	frost	fog	brightness	contrast	elastic-transform	pixelate
shot-noise	0													
impulse-noise	0	0												
defocus-blur	0	0	0											
glass-blur	0	0	0	0										
motion-blur	0	0	0	0	0									
zoom-blur	0	0	0	0	0	0								
snow	0	0	0	0	0	0	0							
frost	0	0	0	0.181	0	0	0	0						
fog	0	0	0	0	0	0	0	0	0					
brightness	0	0	0	0	0	0	0	0	0	0				
contrast	0	0	0	0	0	0	0	0	0	0	0			
elastic-transform	0	0	0	0	0	0	0	0	0	0	0	0		
pixelate	0	0	0	0	0	0	0	0	0	0	0	0	0	
jpeg-compression	0	0	0	0	0	0	0	0	0	0	0	0	0	0.756

Table 30: AP. Pairwise Wilcox test with Bonferroni correction for corruption on Azure and UTK

	gaussian-noise	shot-noise	impulse-noise	defocus-blur	glass-blur	motion-blur	zoom-blur	snow	frost	fog	brightness	contrast	elastic-transform	pixelate
shot-noise	0													
impulse-noise	0.272	0												
defocus-blur	0	0	0											
glass-blur	0	0	0	0										
motion-blur	0	0	0	0	0									
zoom-blur	0	0	0	0	0	0								
snow	0	0	0	0	0	0	0							
frost	0	0	0	0	0	0	0	0.272						
fog	0	0	0	0	0	0	0	0	0					
brightness	0	0	0	0	0	0	0	0	0	0				
contrast	0	0	0	0	0	0	0	0	0	0	0			
elastic-transform	0	0	0	0	0	0	0	0	0	0	0	0		
pixelate	0	0	0	0	0	0	0	0	0	0.084	0	0	0	
jpeg-compression	0	0	0	0	0	0	0	0	0	0	0	0	0	0

Table 31: AP. Pairwise Wilcox test with Bonferroni correction for corruption on GCP and UTK

	gaussian-noise	shot-noise	impulse-noise	defocus-blur	glass-blur	motion-blur	zoom-blur	snow	frost	fog	brightness	contrast	elastic-transform	pixelate
shot-noise	0													
impulse-noise	0	0												
defocus-blur	0	0	0											
glass-blur	0	0	0	0.003										
motion-blur	0	0	0	0	0									
zoom-blur	0	0	0	0	0	0								
snow	0.357	0	0	0	0	0	0							
frost	0	0	0	0	0	0	0	0						
fog	0	0	0	0	0	0	0	0	0					
brightness	0	0	0	0	0	0	0	0	0	0				
contrast	0	0	0	0	0	0	0	0	0.001	0	0			
elastic-transform	0	0	0	0	0	0	0	0	0	0	0	0		
pixelate	0	0	0	0	0	0	0	0	0	0	0	0	0	
jpeg-compression	0	0	0	0	0	0	0	0	0	0	0	0	0	0

AP p -values for pairwise Wilcox test with Bonferroni correction for corruption on MogFace and UTK can be found in Table 32

Table 32: AP. Pairwise Wilcox test with Bonferroni correction for corruption on MogFace and UTK

	gaussian-noise	shot-noise	impulse-noise	defocus-blur	glass-blur	motion-blur	zoom-blur	snow	frost	fog	brightness	contrast	elastic-transform	pixelate
shot-noise	0													
impulse-noise	0	0												
defocus-blur	0	0	0											
glass-blur	0	0	0	0										
motion-blur	0	0	0	0	0									
zoom-blur	0	0	0	0	0	0								
snow	0	0	0	0	0	0	0							
frost	0	0	0	0	0	0	0	0						
fog	0	0	0	0	0	0	0	0	0					
brightness	0	0	0	0	0	0	0	0	0	0				
contrast	0	0	0	0	0	0	0	0	0	0	0			
elastic-transform	0	0	0	0	0	0	0	0	0	0	0	0		
pixelate	0	0	0	0	0	0	0	0	0	0	0	0	0	
jpeg-compression	0	0	0	0	0	0	0	0	0	0	0	0	0	0

AP p -values for pairwise Wilcox test with Bonferroni correction for corruption on TinaFace and UTK can be found in Table 33

Table 33: AP. Pairwise Wilcox test with Bonferroni correction for corruption on TinaFace and UTK

	gaussian-noise	shot-noise	impulse-noise	defocus-blur	glass-blur	motion-blur	zoom-blur	snow	frost	fog	brightness	contrast	elastic-transform	pixelate
shot-noise	0													
impulse-noise	0	0												
defocus-blur	0	0	0											
glass-blur	0	0	0	0										
motion-blur	0	0	0	0	0									
zoom-blur	0	0	0	0	0	0								
snow	0	0	0	0	0	0	0							
frost	0	0	0	0	0	0	0	0						
fog	0	0	0	0	0	0	0	0	0					
brightness	0	0	0	0	0	0	0	0	0	0				
contrast	0	0	0	0	0	0	0	0	0	0	0			
elastic-transform	0	0	0	0	0	0	0	0	0	0	0	0		
pixelate	0	0	0	0.031	0	0	0	0	0	0	0	0	0	
jpeg-compression	0	0	0	0	0	0	0	0	0	0	0	0	0	0

AP p -values for pairwise Wilcox test with Bonferroni correction for corruption on Yolov5 and UTK can be found in Table 34

Table 34: AP. Pairwise Wilcox test with Bonferroni correction for corruption on Yolov5 and UTK

	gaussian-noise	shot-noise	impulse-noise	defocus-blur	glass-blur	motion-blur	zoom-blur	snow	frost	fog	brightness	contrast	elastic-transform	pixelate
shot-noise	0													
impulse-noise	0	0												
defocus-blur	0	0	0											
glass-blur	0	0	0	0										
motion-blur	0	0	0	0	0									
zoom-blur	0	0	0	0	0	0								
snow	0	0	0	0	0	0	0							
frost	0	0	0	0	0	0	0	0						
fog	0	0	0	0	0	0	0	0	0					
brightness	0	0	0	0	0	0	0	0	0	0				
contrast	0	0	0	0	0	0	0	0	0	0	0			
elastic-transform	0	0	0	0	0	0	0	0	0	0	0	0		
pixelate	0	0	0	0	0	0	0	0	0	0	0	0	0	
jpeg-compression	0	0	0	0	0	0	0	0	0	0	0	0.010	0	0

D.3 AP — Age Comparison Claims

AP p -values for pairwise Wilcox test with Bonferroni correction for Age on AWS and Adience can be found in Table 35

Table 35: AP. Pairwise Wilcox test with Bonferroni correction for Age on AWS and Adience

	0-2	3-7	8-14	15-24	25-35	36-45	46-59
3-7	0						
8-14	0	0					
15-24	0	0	0				
25-35	0	0	0	0			
36-45	0	0	0	0	0		
46-59	0	0.00000	0	0	0	0	
60+	0	0	0	0	0	0	0

AP p -values for pairwise Wilcox test with Bonferroni correction for Age on Azure and Adience can be found in Table 36

Table 36: AP. Pairwise Wilcox test with Bonferroni correction for Age on Azure and Adience

	0-2	3-7	8-14	15-24	25-35	36-45	46-59
3-7	0						
8-14	0	0					
15-24	0	0	0				
25-35	0	0	0	0			
36-45	0	0.00000	0	0	0.00000		
46-59	0	0.118	0	0	0	0	
60+	0	0	0	0	0	0	0

AP p -values for pairwise Wilcox test with Bonferroni correction for Age on GCP and Adience can be found in Table 37

AP p -values for pairwise Wilcox test with Bonferroni correction for Age on MogFace and Adience can be found in Table 38

Table 37: AP. Pairwise Wilcox test with Bonferroni correction for Age on GCP and Adience

	0-2	3-7	8-14	15-24	25-35	36-45	46-59
3-7	0						
8-14	0	0					
15-24	0	0.00004	0				
25-35	0	0	0	0.134			
36-45	0.008	0	0	0	0		
46-59	0	0	0	0	0	0	
60+	0	0	0	0	0	0	0.003

Table 38: AP. Pairwise Wilcox test with Bonferroni correction for Age on MogFace and Adience

	0-2	3-7	8-14	15-24	25-35	36-45	46-59
3-7	0						
8-14	0	0					
15-24	0	0	0.945				
25-35	0	0	0.001	0.003			
36-45	0	0	0	0	0		
46-59	0	0.524	0	0	0	0	
60+	0.198	0	0	0	0	0	0

AP p -values for pairwise Wilcox test with Bonferroni correction for Age on TinaFace and Adience can be found in Table 39

Table 39: AP. Pairwise Wilcox test with Bonferroni correction for Age on TinaFace and Adience

	0-2	3-7	8-14	15-24	25-35	36-45	46-59
3-7	0						
8-14	0	0					
15-24	0	0	0				
25-35	0	0	0	0			
36-45	0	0	0.0001	0	0		
46-59	0	0	0.005	0	0	0	
60+	0.010	0	0	0	0	0	0

AP p -values for pairwise Wilcox test with Bonferroni correction for Age on Yolov5 and Adience can be found in Table 40

Table 40: AP. Pairwise Wilcox test with Bonferroni correction for Age on Yolov5 and Adience

	0-2	3-7	8-14	15-24	25-35	36-45	46-59
3-7	0.226						
8-14	0	0					
15-24	0	0.00000	0.00000				
25-35	0.00000	0.0001	0	0.049			
36-45	0	0	0	0	0		
46-59	0	0	0.0002	0	0	0.0001	
60+	0	0	0	0	0	0	0

AP p -values for pairwise Wilcox test with Bonferroni correction for Age on AWS and CCD can be found in Table 41

AP p -values for pairwise Wilcox test with Bonferroni correction for Age on Azure and CCD can be found in Table 42

Table 41: AP. Pairwise Wilcox test with Bonferroni correction for Age on AWS and CCD

	19-45	45-64
45-64	0	
65+	0	0

Table 42: AP. Pairwise Wilcox test with Bonferroni correction for Age on Azure and CCD

	19-45	45-64
45-64	0	
65+	0	0

AP p -values for pairwise Wilcox test with Bonferroni correction for Age on GCP and CCD can be found in Table 43

Table 43: AP. Pairwise Wilcox test with Bonferroni correction for Age on GCP and CCD

	19-45	45-64
45-64	0	
65+	0	0

AP p -values for pairwise Wilcox test with Bonferroni correction for Age on MogFace and CCD can be found in Table 44

Table 44: AP. Pairwise Wilcox test with Bonferroni correction for Age on MogFace and CCD

	19-45	45-64
45-64	0	
65+	0	0

AP p -values for pairwise Wilcox test with Bonferroni correction for Age on TinaFace and CCD can be found in Table 45

Table 45: AP. Pairwise Wilcox test with Bonferroni correction for Age on TinaFace and CCD

	19-45	45-64
45-64	0	
65+	0	0

AP p -values for pairwise Wilcox test with Bonferroni correction for Age on Yolov5 and CCD can be found in Table 46

Table 46: AP. Pairwise Wilcox test with Bonferroni correction for Age on Yolov5 and CCD

	19-45	45-64
45-64	0	
65+	0	0

AP p -values for pairwise Wilcox test with Bonferroni correction for Age on AWS and MIAP can be found in Table 47

AP p -values for pairwise Wilcox test with Bonferroni correction for Age on Azure and MIAP can be found in Table 48

AP p -values for pairwise Wilcox test with Bonferroni correction for Age on GCP and MIAP can be found in Table 49

Table 47: AP. Pairwise Wilcox test with Bonferroni correction for Age on AWS and MIAP

	Young	Middle	Older
Middle	0		
Older	0	0	
Unknown	0	0	0

Table 48: AP. Pairwise Wilcox test with Bonferroni correction for Age on Azure and MIAP

	Young	Middle	Older
Middle	0		
Older	0	0	
Unknown	0	0.00000	0

Table 49: AP. Pairwise Wilcox test with Bonferroni correction for Age on GCP and MIAP

	Young	Middle	Older
Middle	0		
Older	0	0	
Unknown	0	0	0

AP p -values for pairwise Wilcox test with Bonferroni correction for Age on MogFace and MIAP can be found in Table 50

Table 50: AP. Pairwise Wilcox test with Bonferroni correction for Age on MogFace and MIAP

	Young	Middle	Older
Middle	0		
Older	0	0	
Unknown	0	0.00000	0

AP p -values for pairwise Wilcox test with Bonferroni correction for Age on TinaFace and MIAP can be found in Table 51

Table 51: AP. Pairwise Wilcox test with Bonferroni correction for Age on TinaFace and MIAP

	Young	Middle	Older
Middle	0		
Older	0	0	
Unknown	0	0.001	0

AP p -values for pairwise Wilcox test with Bonferroni correction for Age on Yolov5 and MIAP can be found in Table 52

Table 52: AP. Pairwise Wilcox test with Bonferroni correction for Age on Yolov5 and MIAP

	Young	Middle	Older
Middle	0		
Older	0	0	
Unknown	0	0	0

AP p -values for pairwise Wilcox test with Bonferroni correction for Age on AWS and UTK can be found in Table 53

Table 53: AP. Pairwise Wilcoxon test with Bonferroni correction for Age on AWS and UTK

	0-18	19-45	45-64
19-45	0		
45-64	0	0	
65+	0	0	0

AP p -values for pairwise Wilcoxon test with Bonferroni correction for Age on Azure and UTK can be found in Table 54

Table 54: AP. Pairwise Wilcoxon test with Bonferroni correction for Age on Azure and UTK

	0-18	19-45	45-64
19-45	0		
45-64	0	0.570	
65+	0	0	0

AP p -values for pairwise Wilcoxon test with Bonferroni correction for Age on GCP and UTK can be found in Table 55

Table 55: AP. Pairwise Wilcoxon test with Bonferroni correction for Age on GCP and UTK

	0-18	19-45	45-64
19-45	0		
45-64	0	0	
65+	0	0	0

AP p -values for pairwise Wilcoxon test with Bonferroni correction for Age on MogFace and UTK can be found in Table 56

Table 56: AP. Pairwise Wilcoxon test with Bonferroni correction for Age on MogFace and UTK

	0-18	19-45	45-64
19-45	0		
45-64	0	0	
65+	0	0	0

AP p -values for pairwise Wilcoxon test with Bonferroni correction for Age on TinaFace and UTK can be found in Table 57

Table 57: AP. Pairwise Wilcoxon test with Bonferroni correction for Age on TinaFace and UTK

	0-18	19-45	45-64
19-45	0		
45-64	0.00000	0	
65+	0	0	0

AP p -values for pairwise Wilcoxon test with Bonferroni correction for Age on Yolov5 and UTK can be found in Table 58

D.4 AP — Gender Comparison Claims

AP p -values for pairwise Wilcoxon test with Bonferroni correction for Gender on AWS and Adience can be found in Table 59

AP p -values for pairwise Wilcoxon test with Bonferroni correction for Gender on Azure and Adience can be found in Table 60

Table 58: AP. Pairwise Wilcox test with Bonferroni correction for Age on Yolov5 and UTK

	0-18	19-45	45-64
19-45	0		
45-64	0	0	
65+	0	0	0

Table 59: AP. Pairwise Wilcox test with Bonferroni correction for Gender on AWS and Adience

	Female
Male	0

Table 60: AP. Pairwise Wilcox test with Bonferroni correction for Gender on Azure and Adience

	Female
Male	0

AP p -values for pairwise Wilcox test with Bonferroni correction for Gender on GCP and Adience can be found in Table 61

Table 61: AP. Pairwise Wilcox test with Bonferroni correction for Gender on GCP and Adience

	Female
Male	0

AP p -values for pairwise Wilcox test with Bonferroni correction for Gender on MogFace and Adience can be found in Table 62

Table 62: AP. Pairwise Wilcox test with Bonferroni correction for Gender on MogFace and Adience

	Female
Male	0

AP p -values for pairwise Wilcox test with Bonferroni correction for Gender on TinaFace and Adience can be found in Table 63

Table 63: AP. Pairwise Wilcox test with Bonferroni correction for Gender on TinaFace and Adience

	Female
Male	0.203

AP p -values for pairwise Wilcox test with Bonferroni correction for Gender on Yolov5 and Adience can be found in Table 64

Table 64: AP. Pairwise Wilcox test with Bonferroni correction for Gender on Yolov5 and Adience

	Female
Male	0

AP p -values for pairwise Wilcox test with Bonferroni correction for Gender on AWS and CCD can be found in Table 65

AP p -values for pairwise Wilcox test with Bonferroni correction for Gender on Azure and CCD can be found in Table 66

Table 65: AP. Pairwise Wilcox test with Bonferroni correction for Gender on AWS and CCD

	Female	Male
Male	0	
Other	0.680	0

Table 66: AP. Pairwise Wilcox test with Bonferroni correction for Gender on Azure and CCD

	Female	Male
Male	0	
Other	0.171	0

AP p -values for pairwise Wilcox test with Bonferroni correction for Gender on GCP and CCD can be found in Table 67

Table 67: AP. Pairwise Wilcox test with Bonferroni correction for Gender on GCP and CCD

	Female	Male
Male	0	
Other	0.003	0

AP p -values for pairwise Wilcox test with Bonferroni correction for Gender on MogFace and CCD can be found in Table 68

Table 68: AP. Pairwise Wilcox test with Bonferroni correction for Gender on MogFace and CCD

	Female	Male
Male	0	
Other	0.806	0

AP p -values for pairwise Wilcox test with Bonferroni correction for Gender on TinaFace and CCD can be found in Table 69

Table 69: AP. Pairwise Wilcox test with Bonferroni correction for Gender on TinaFace and CCD

	Female	Male
Male	0	
Other	0.740	0

AP p -values for pairwise Wilcox test with Bonferroni correction for Gender on Yolov5 and CCD can be found in Table 70

Table 70: AP. Pairwise Wilcox test with Bonferroni correction for Gender on Yolov5 and CCD

	Female	Male
Male	0	
Other	0	0

AP p -values for pairwise Wilcox test with Bonferroni correction for Gender on AWS and MIAP can be found in Table 71

AP p -values for pairwise Wilcox test with Bonferroni correction for Gender on Azure and MIAP can be found in Table 72

AP p -values for pairwise Wilcox test with Bonferroni correction for Gender on GCP and MIAP can be found in Table 73

Table 71: AP. Pairwise Wilcox test with Bonferroni correction for Gender on AWS and MIAP

	Predominantly Feminine	Predominantly Masculine
Predominantly Masculine	0	
Unknown	0	0

Table 72: AP. Pairwise Wilcox test with Bonferroni correction for Gender on Azure and MIAP

	Predominantly Feminine	Predominantly Masculine
Predominantly Masculine	0	
Unknown	0	0

Table 73: AP. Pairwise Wilcox test with Bonferroni correction for Gender on GCP and MIAP

	Predominantly Feminine	Predominantly Masculine
Predominantly Masculine	0	
Unknown	0	0

AP p -values for pairwise Wilcox test with Bonferroni correction for Gender on MogFace and MIAP can be found in Table 74

Table 74: AP. Pairwise Wilcox test with Bonferroni correction for Gender on MogFace and MIAP

	Predominantly Feminine	Predominantly Masculine
Predominantly Masculine	0	
Unknown	0	0

AP p -values for pairwise Wilcox test with Bonferroni correction for Gender on TinaFace and MIAP can be found in Table 75

Table 75: AP. Pairwise Wilcox test with Bonferroni correction for Gender on TinaFace and MIAP

	Predominantly Feminine	Predominantly Masculine
Predominantly Masculine	0	
Unknown	0	0

AP p -values for pairwise Wilcox test with Bonferroni correction for Gender on Yolov5 and MIAP can be found in Table 76

Table 76: AP. Pairwise Wilcox test with Bonferroni correction for Gender on Yolov5 and MIAP

	Predominantly Feminine	Predominantly Masculine
Predominantly Masculine	0	
Unknown	0	0

AP p -values for pairwise Wilcox test with Bonferroni correction for Gender on AWS and UTK can be found in Table 77

Table 77: AP. Pairwise Wilcox test with Bonferroni correction for Gender on AWS and UTK

	Female
Male	0

AP p -values for pairwise Wilcoxon test with Bonferroni correction for Gender on Azure and UTK can be found in Table 78

Table 78: AP. Pairwise Wilcoxon test with Bonferroni correction for Gender on Azure and UTK

	Female
Male	0

AP p -values for pairwise Wilcoxon test with Bonferroni correction for Gender on GCP and UTK can be found in Table 79

Table 79: AP. Pairwise Wilcoxon test with Bonferroni correction for Gender on GCP and UTK

	Female
Male	0

AP p -values for pairwise Wilcoxon test with Bonferroni correction for Gender on MogFace and UTK can be found in Table 80

Table 80: AP. Pairwise Wilcoxon test with Bonferroni correction for Gender on MogFace and UTK

	Female
Male	0.0001

AP p -values for pairwise Wilcoxon test with Bonferroni correction for Gender on TinaFace and UTK can be found in Table 81

Table 81: AP. Pairwise Wilcoxon test with Bonferroni correction for Gender on TinaFace and UTK

	Female
Male	0

AP p -values for pairwise Wilcoxon test with Bonferroni correction for Gender on Yolov5 and UTK can be found in Table 82

Table 82: AP. Pairwise Wilcoxon test with Bonferroni correction for Gender on Yolov5 and UTK

	Female
Male	0

D.5 AP — Skin Type Comparison Claims

AP p -values for pairwise Wilcoxon test with Bonferroni correction for Skin Type on AWS and CCD can be found in Table 83

Table 83: AP. Pairwise Wilcoxon test with Bonferroni correction for Skin Type on AWS and CCD

	Light Fitz
Dark Fitz	0

AP p -values for pairwise Wilcoxon test with Bonferroni correction for Skin Type on Azure and CCD can be found in Table 84

AP p -values for pairwise Wilcoxon test with Bonferroni correction for Skin Type on GCP and CCD can be found in Table 85

Table 84: AP. Pairwise Wilcox test with Bonferroni correction for Skin Type on Azure and CCD

	Light Fitz
Dark Fitz	0

Table 85: AP. Pairwise Wilcox test with Bonferroni correction for Skin Type on GCP and CCD

	Light Fitz
Dark Fitz	0

Table 86: AP. Pairwise Wilcox test with Bonferroni correction for Skin Type on MogFace and CCD

	Light Fitz
Dark Fitz	0

AP p -values for pairwise Wilcox test with Bonferroni correction for Skin Type on MogFace and CCD can be found in Table 86

AP p -values for pairwise Wilcox test with Bonferroni correction for Skin Type on TinaFace and CCD can be found in Table 87

Table 87: AP. Pairwise Wilcox test with Bonferroni correction for Skin Type on TinaFace and CCD

	Light Fitz
Dark Fitz	0

AP p -values for pairwise Wilcox test with Bonferroni correction for Skin Type on Yolov5 and CCD can be found in Table 88

Table 88: AP. Pairwise Wilcox test with Bonferroni correction for Skin Type on Yolov5 and CCD

	Light Fitz
Dark Fitz	0

AP p -values for pairwise Wilcox test with Bonferroni correction for Skin Type and the interaction with Lighting on AWS and CCD can be found in Table 89

Table 89: AP. Pairwise Wilcox test with Bonferroni correction for Skin Type and the interaction with Lighting on AWS and CCD

	Dark Fitz+Bright	Dark Fitz+Dim	Light Fitz+Bright
Dark Fitz+Dim	0		
Light Fitz+Bright	0	0	
Light Fitz+Dim	0	0.567	0

AP p -values for pairwise Wilcox test with Bonferroni correction for Skin Type and the interaction with Lighting on Azure and CCD can be found in Table 90

AP p -values for pairwise Wilcox test with Bonferroni correction for Skin Type and the interaction with Lighting on GCP and CCD can be found in Table 91

AP p -values for pairwise Wilcox test with Bonferroni correction for Skin Type and the interaction with Lighting on MogFace and CCD can be found in Table 92

AP p -values for pairwise Wilcox test with Bonferroni correction for Skin Type and the interaction with Lighting on TinaFace and CCD can be found in Table 93

Table 90: AP. Pairwise Wilcoxon test with Bonferroni correction for Skin Type and the interaction with Lighting on Azure and CCD

	Dark Fitz+Bright	Dark Fitz+Dim	Light Fitz+Bright
Dark Fitz+Dim	0		
Light Fitz+Bright	0	0	
Light Fitz+Dim	0	0.076	0

Table 91: AP. Pairwise Wilcoxon test with Bonferroni correction for Skin Type and the interaction with Lighting on GCP and CCD

	Dark Fitz+Bright	Dark Fitz+Dim	Light Fitz+Bright
Dark Fitz+Dim	0		
Light Fitz+Bright	0	0	
Light Fitz+Dim	0	0	0

Table 92: AP. Pairwise Wilcoxon test with Bonferroni correction for Skin Type and the interaction with Lighting on MogFace and CCD

	Dark Fitz+Bright	Dark Fitz+Dim	Light Fitz+Bright
Dark Fitz+Dim	0		
Light Fitz+Bright	0	0	
Light Fitz+Dim	0	0.316	0

Table 93: AP. Pairwise Wilcoxon test with Bonferroni correction for Skin Type and the interaction with Lighting on TinaFace and CCD

	Dark Fitz+Bright	Dark Fitz+Dim	Light Fitz+Bright
Dark Fitz+Dim	0		
Light Fitz+Bright	0	0	
Light Fitz+Dim	0	0.004	0

AP p-values for pairwise Wilcoxon test with Bonferroni correction for Skin Type and the interaction with Lighting on Yolov5 and CCD can be found in Table 94

Table 94: AP. Pairwise Wilcoxon test with Bonferroni correction for Skin Type and the interaction with Lighting on Yolov5 and CCD

	Dark Fitz+Bright	Dark Fitz+Dim	Light Fitz+Bright
Dark Fitz+Dim	0		
Light Fitz+Bright	0	0	
Light Fitz+Dim	0	0.00004	0

AP p-values for pairwise Wilcoxon test with Bonferroni correction for Skin Type and the interaction with Age and Gender on AWS and CCD can be found in Table 95

Table 95: AP. Pairwise Wilcoxon test with Bonferroni correction for Skin Type and the interaction with Age and Gender on AWS and CCD

	Dark Fitz+Bright	Dark Fitz+Dim	Light Fitz+Bright
Dark Fitz+Dim	0		
Light Fitz+Bright	0	0	
Light Fitz+Dim	0	0.00004	0

AP p-values for pairwise Wilcoxon test with Bonferroni correction for Skin Type and the interaction with Age and Gender on Azure and CCD can be found in Table 96

Table 102: AP. Pairwise Wilcox test with Bonferroni correction for Lighting on Azure and CCD

	Bright
Dim	0

AP p -values for pairwise Wilcox test with Bonferroni correction for Lighting on GCP and CCD can be found in Table 103

Table 103: AP. Pairwise Wilcox test with Bonferroni correction for Lighting on GCP and CCD

	Bright
Dim	0

AP p -values for pairwise Wilcox test with Bonferroni correction for Lighting on MogFace and CCD can be found in Table 104

Table 104: AP. Pairwise Wilcox test with Bonferroni correction for Lighting on MogFace and CCD

	Bright
Dim	0

AP p -values for pairwise Wilcox test with Bonferroni correction for Lighting on TinaFace and CCD can be found in Table 105

Table 105: AP. Pairwise Wilcox test with Bonferroni correction for Lighting on TinaFace and CCD

	Bright
Dim	0

AP p -values for pairwise Wilcox test with Bonferroni correction for Lighting on Yolov5 and CCD can be found in Table 106

Table 106: AP. Pairwise Wilcox test with Bonferroni correction for Lighting on Yolov5 and CCD

	Bright
Dim	0